

This dissertation has been
microfilmed exactly as received 66-15,259

NOWATZKI, Edward Alexander, 1936-
FABRIC CHANGES ACCOMPANYING SHEAR STRAINS
IN A COHESIVE SOIL.

University of Arizona, Ph.D., 1966
Engineering, civil

University Microfilms, Inc., Ann Arbor, Michigan

© COPYRIGHTED

BY

EDWARD ALEXANDER NOWATZKI

1967

FABRIC CHANGES ACCOMPANYING SHEAR STRAINS
IN A COHESIVE SOIL

by

Edward Alexander Nowatzki

A Dissertation Submitted to the Faculty of the
DEPARTMENT OF CIVIL ENGINEERING
In Partial Fulfillment of the Requirements
For the Degree of
DOCTOR OF PHILOSOPHY
In the Graduate College
THE UNIVERSITY OF ARIZONA

1966

THE UNIVERSITY OF ARIZONA
GRADUATE COLLEGE

I hereby recommend that this dissertation prepared under my
direction by Edward Alexander Nowatzki
entitled FABRIC CHANGES ACCOMPANYING SHEAR STRAINS
IN A COHESIVE SOIL
be accepted as fulfilling the dissertation requirement of the
degree of Doctor of Philosophy

Richard L. Sloan
Dissertation Director

22 June 1966
Date

After inspection of the dissertation, the following members
of the Final Examination Committee concur in its approval and
recommend its acceptance:*

<u>G. C. Lacy</u>	<u>6/23/66</u>
<u>E. M. Laurson</u>	<u>6/25/66</u>
<u>J. R. Browning</u>	<u>6/29/66</u>
<u>G. A. Jumenty</u>	<u>6/29/66</u>
<u>John M. Guilbert</u>	<u>7/14/66</u>

*This approval and acceptance is contingent on the candidate's
adequate performance and defense of this dissertation at the
final oral examination. The inclusion of this sheet bound into
the library copy of the dissertation is evidence of satisfactory
performance at the final examination.

PLEASE NOTE:
Figure pages are not original
copy. They tend to "curl".
Filmed in the best possible
way.

University Microfilms, Inc.

STATEMENT BY AUTHOR

This dissertation has been submitted in partial fulfillment of requirements for an advanced degree at The University of Arizona and is deposited in the University Library to be made available to borrowers under rules of the Library.

Brief quotations from this dissertation are allowable without special permission, provided that accurate acknowledgment of source is made. Requests for permission for extended quotation from or reproduction of this manuscript in whole or in part may be granted by the copyright holder.

SIGNED: Edward Alexander Nowatzki

ACKNOWLEDGMENT

The author wishes to acknowledge the invaluable assistance of his dissertation director, Professor Richard L. Sloane, in every phase of this research. His criticisms and suggestions are appreciated second only to his patience.

Words cannot adequately express the acknowledgment the author wishes to extend to his wife, Patricia, for her consolation and inspiration at the times when these were needed mostly. It is to her and to our children, Christopher and Eileen, that I wish to dedicate this dissertation.

TABLE OF CONTENTS

	Page
LIST OF ILLUSTRATIONS.....	vii
LIST OF TABLES.....	viii
ABSTRACT.....	ix
CHAPTER I INTRODUCTION.....	1
Background.....	1
Statement of the Problem.....	2
Review of Literature.....	3
Scope.....	19
CHAPTER II METHODS OF LABORATORY INVESTIGATION.....	21
The Cohesive Material Studied.....	21
Sample Preparation - Compaction Curve.....	21
Sample Preparation - Direct Shear.....	24
Direct Shear Tests.....	27
X-ray Diffraction Study.....	32
Electron Microscope Study.....	38
CHAPTER III PRESENTATION AND DISCUSSION OF RESULTS.....	45
General.....	45
Preliminary Investigations.....	45
The Moisture - Density Relationship.....	45
The Shear Stress-Strain Relationships.....	46
The X-ray Diffraction Study.....	47
The Electron Microscope Study.....	55
A Presentation of the Electron Micrographs...	55
Qualitative and Quantitative Analysis of the Shear Zone.....	61
Correlation of Electron Micrographs with X-ray Diffraction Data.....	70

TABLE OF CONTENTS - Continued

	Page
CHAPTER IV	
CONCLUSIONS AND RECOMMENDATIONS FOR FURTHER STUDY.....	74
Conclusions.....	74
Recommendations for Further Study.....	76
APPENDIX A	
TABLES RELATING TO PHYSICAL PROPERTIES OF HYDRITE UF.....	78
APPENDIX B	
TABLE OF PERTINENT X-RAY DIFFRACTION DATA.....	80
APPENDIX C	
BASIS FOR NON-LINEAR NOMINAL STRAIN DISTRIBUTION IN A CIRCULAR SHEAR SPECIMEN.....	82
LIST OF REFERENCES.....	84

LIST OF ILLUSTRATIONS

Figure		Page
1.	Goldschmidt-Lambe Concept of Clay Fabric.....	7
2.	Effect of Compaction on Clay Fabric (Lambe)....	9
3.	Book-Clay Packet Analogy (Kell).....	11
4.	Static Compaction Curve For Hydrite UF at a Compactive Effort of 500 lbs/sq in.....	23
5.	Procedure For Cutting Shear Samples.....	28
6.	Shear Stress Versus Nominal Shearing Strain For Various Normal Loads.....	31
7.	Procedure For Cutting X-ray Diffraction Specimens.....	33
8.	Primary and Secondary Replication and Mounting Procedure.....	41
9.	Variation of Orientation Index With Per Cent of Failure Strain - Vertical Specimens.....	51
10.	Variation of Orientation Index With Per Cent of Failure Strain - Horizontal Specimens.....	52
11.	Kaolinite Fabric - Initial Condition.....	56
12.	Kaolinite Fabric - 25 Per Cent of Failure Strain.....	57
13.	Kaolinite Fabric - 50 Per Cent of Failure Strain.....	58
14.	Kaolinite Fabric - 75 Per Cent of Failure Strain.....	59
15.	Kaolinite Fabric - Failure Condition.....	60
16.	Vertical Fabric Reorientation Due to Increasing Shear Strain.....	75
17.	Non-linear Nominal Strain Distribution in a Circular Specimen.....	83

LIST OF TABLES

Table		Page
1.	Physical Properties of Hydrite UF.....	78
2.	Molding Moisture Content and Dry Density Values for Kaolinite Shear Samples.....	79
3.	Average Orientation Indices for Both Carbowax- Impregnated Test Specimens and Non-Impregnated Control Specimens.....	49
4.	Pertinent Results Computed From Peak Counts for Both Carbowax-Impregnated Test Specimens and Non-Impregnated Control Specimens.....	80
5.	Approximate Size of Shear Zone Along Vertical Diametrical Plane Parallel to Applied Shear Load.....	62

ABSTRACT

Kaolinite specimens were statically compacted dry of optimum moisture content to obtain an initially randomly-oriented fabric. A series of direct-shear failure-tests were performed at four different normal loads and at a low rate of shear strain. The strain corresponding to peak shear stress was defined as the failure strain. Three percentages of the nominal failure strain were computed for each normal load and specimens strained to these values. Immediately following strain in direct shear, the specimens were Carbowax-impregnated. After the Carbowax had hardened, both vertical and horizontal sections were cut from each strain specimen, surface-finished, and subjected to x-ray diffraction. A ratio was taken of the average net peak-intensity count at the (020) peak to the average net peak-intensity count at the (002) peak to quantitatively describe the fabric at a given per cent of failure strain. This ratio is defined as the orientation index.

At the completion of the x-ray diffraction study, specimens from one normal-load series were etched and two-stage replicated. The final carbon replicas were viewed in the electron microscope. Special finder grids preserved the orientation of the replica with respect to the top and front of the strained specimen, and allowed orientation studies to

be made. An hypothesis of the mechanisms responsible for fabric reaction to shear strains was evolved from a consideration of the energy states of particles or groups of particles within the affected area.

It is shown that a reorientation of fabric from random to parallel occurs in a partially-saturated kaolinite with increase in shear strain. The reorientation takes place through the formation of a series of individually-oriented zones within the gross shear zone in both the vertical and horizontal planes. It is also shown that the vertical extent of the gross shear zone is almost fully established between 25 and 50 per cent of failure strain and that, at failure, it measures approximately 1.5 cm. The horizontal extent of the gross shear zone is fully established before 25 per cent of failure strain and extends throughout the specimen.

Finally, an analysis shows that three-dimensional influences could have caused x-ray data to indicate a reverse trend toward randomness with increase in strain. The apparent contradiction between x-ray diffraction and electron microscopy evidence concerning the direction in which fabric changes proceed with increase in shear is resolved.

CHAPTER I

INTRODUCTION

Background

In soil mechanics, derived from solid mechanics concepts, certain soil properties such as: permeability, internal friction, cohesion, compressibility, shear strength, etc., are designated as the "fundamental" soil properties. In the derivation of the relationships between these "fundamental" properties and the physical, observed behavior of soil an assumption of homogeneity is made. In actuality soil is a three-phase system consisting of solids, liquid and gas. The interaction of the properties of each of the members of the three-phase soil system with the others is physically expressed in the one truly fundamental property of any clay soil, namely, soil fabric or the overall arrangement of clay platelets or groups (books, packets) of clay platelets within the soil mass. In the words of R.E.Olsen (1963), "The engineering properties of cohesive soils are the physical manifestation of complex physico-chemical interactions between particles".

It is this "complex physico-chemical interaction between particles" that determines the fabric of a soil,

and the common physical properties are merely measurements of the reactions of the fabric to certain mechanical and external stimuli. These reactions have been arbitrarily chosen as standards for the practical solution of soils problems. One such reaction is the property known as shear strength.

In the past, the strength properties of cohesive soils have been examined from a strictly mechanical viewpoint. The direct result of this approach has been the development of an exhaustive testing of apparatus rather than soil, because equipment inadequacies have placed major restrictions on the evaluation of test results. Recently, a trend has been developing away from such a mechanical or macro-analysis toward a more fundamental mechanico-chemical or micro-analysis of the mechanisms responsible for shear strength in saturated clay soils. With a more complete understanding of the shearing process on a micro-level, a deeper knowledge of the factors affecting the physical manifestation (shear strength) of these micro-reactions will be obtained.

Statement of the Problem

The results of previous research in this area have shown that the fabric of a clay soil governs all of its mechanical properties. It will be the object of this study to investigate the effect of shear strain on the fabric of a partially-saturated clay and to correlate any changes of

fabric accompanying the applied shear strains with the physical shear strength of the soil.

Review of Literature

For the sake of clarity the historical development of the present theory of clay soil fabric will be reviewed precedent to a review of the current theory on the development of shearing resistance in saturated clay soils and the mechanisms that occur in the shearing process. This is done because the latter relies heavily on fundamental concepts contained in the former.

According to Arthur Casagrande (1932) the concept of soil micro-structure originated with Karl Terzaghi as early as 1925. In his classic work, Erdbaumechanik, auf Bodenphysickalische Grundlage, Terzaghi (1925) says that soils having a structure consisting of an accumulation of spheres possess "single-grain structure". In addition to this type of structure there is the "honeycomb structure" of loosely deposited silts and muds, the "flocculent structure" of coagulated sediments, and the "crumb structure" of the surface strata of cohesive soils. In a translation of this part of Terzaghi's work by Arthur Casagrande (1960) an explanation of the development of the various types of fabric is given.

Sediments possessing honeycomb structure contain pores which are greater than the largest grains. In flocculent and crumb structure the grains are aggregated in porous lumps which may be considered grains of a

second order of magnitude. The structure of the mass that consists of grains of the second order is in turn either a single-grain or a honeycomb structure of the second order. The flocks are formed immediately upon coagulation of the suspension by an electrolyte and, therefore, the sediment already has a structure of the second order at the time of its formation. The crumbs, however, form in many cases at a later date from soils having single-grain structure under the influence of frost action, of animal and plant life, of salts dissolved in water that is seeping through the soil, and of similar factors.

This concept of clay soil fabric persisted in Civil Engineering until a very late date and can still be found in some texts. At the time Terzaghi presented these "new" concepts to the engineering world, V.M. Goldschmidt was independently developing a more scientifically documented set of conclusions concerning the properties of clay soils and their relation to micro-structure. In particular, Goldschmidt discovered that water or some other liquids of similar properties had to be present besides clay minerals in order for a soil to exhibit cohesive properties. At first it was thought that only liquids with dipole moment could cause cohesion to be developed, however, later investigations by Goldschmidt showed that liquids without any primary dipole moment, such as dioxane, could also have the same property (Rosenqvist, I.Th., 1955). From these observations, Goldschmidt suggested some kind of bond between the mineral phase and the water phase in clay. Faced with the problem of highly sensitive Norwegian "quick" clays, he further theorized that the platelets or flakes of clay minerals in the highly sensitive clays

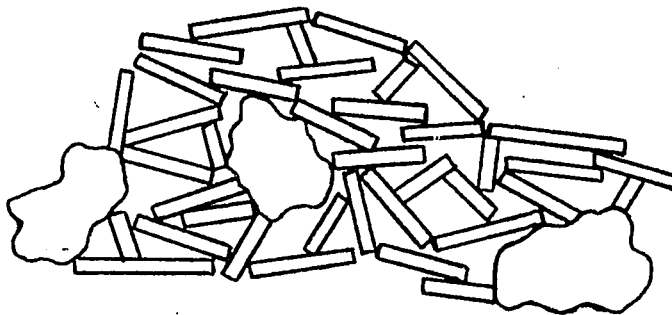
formed a metastable "cardhouse" fabric. The degree of sensitivity was related to the platelet density; the more dense the arrangement, the lower the sensitivity.

Other theories on the structure of cohesive soils were proposed in the years following the work of Terzaghi and Goldschmidt (Russell, 1934; Grim, 1942; and, Winterkorn and Tschebotarioff, 1947) and although most of them were correct and contributed to a deeper understanding of the topic, all, including those of Terzaghi and Goldschmidt, suffered grave inadequacies of incompleteness, generality and oversimplification. It was not until T.W. Lambe (1953) advanced his "working hypothesis" on the structure of inorganic soil that the present day theory of soil fabric and its relation to physical properties began to be more fully developed. It had long been recognized that the most important consideration of soil structure is the nature and magnitude of forces between the soil particles and between soil and water. Lambe went on to describe the possible linkages between the various parts of matter in general. Then, employing these concepts and the principles of colloidal chemistry, he proceeded to explain how the basic unit of soil structure, the soil particles and the eventual soil fabric are progressively built up from atoms, and how the electrokinetic behavior of the soil particles is governed by the principles of colloidal chemistry. Depending upon genetic environment, the resulting structure of an inorganic

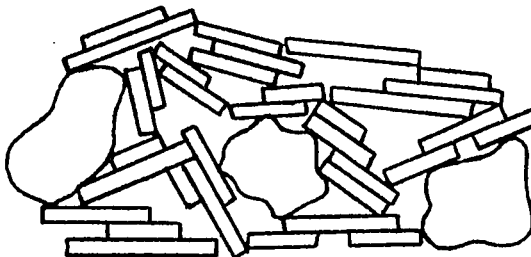
soil could have one of the three basic fabrics postulated by Lambe and shown in Figure 1, Page 7. These represent applications of the theory that a high cation concentration in the pore water, causes the diffuse double layer to collapse. The result is a greater tendency for the positively charged edges of the clay platelets to be attracted to the negatively charged faces of adjacent platelets forming an edge-to-face-contact structure similar to the "cardhouse" structure of Goldschmidt. Conversely, when there is a low cation concentration the diffuse double layer expands, resulting in a greater tendency toward parallelism of clay platelets, at least on a local level. An external mechanical disturbance of sufficient energy would cause a wholesale re-orientation of the fabric in both cases which would result in a generally parallel (oriented) fabric. When examined in the light of experimental data, the first case corresponds to the undisturbed condition of a salt water deposit, the second case to the undisturbed state of a fresh water deposit, and the third case to a remolded condition of both the first and second cases. Using these concepts, Lambe was able to present a more basic explanation of undisturbed and remolded strength.

Lambe further used this concept of soil structure in conjunction with experimental data to explain other soil phenomena such as consolidation, cohesion, secondary compression, thixotropy, etc.

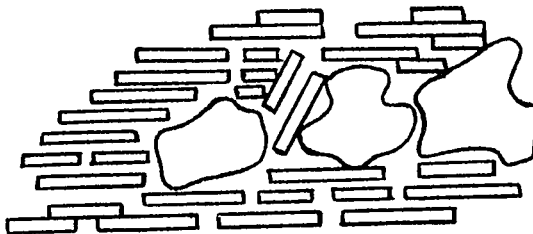
With this foundation firmly established, further



Undisturbed
Salt Water



Undisturbed
Fresh Water



Remolded

Figure 1
Goldschmidt-Lambe Concept
of Clay Fabric

research on this vital subject was initiated and the results extended to a variety of areas of interest to soil engineers (Mitchell, 1956; Bolt, 1956; Tan, 1957; Parry, 1959). One area having significant bearing on the present study is the effect of compaction variables on the fabric of clay. In this regard, Lambe (1958 a; 1958 b) developed a theory of compaction in which the characteristic plot of compacted density versus molding water content (Figure 2, Page 9) was related to fabric through a concept termed "water deficiency". This concept expresses the difference between the amount of water needed by a soil particle at a given state of stress to have a fully developed diffuse double layer and the amount of water available to it.

At W_A (in Figure 2), there is not sufficient water for the diffuse double layers of the soil colloids to develop fully. Actually the small amount of water present at A gives a very high concentration of electrolyte which depresses the double layer. The double layer depression reduces the interparticle repulsion, thereby causing a tendency toward flocculation of the colloids... (which)... generally means a low degree of particle orientation and low density.

Increasing the molding water from W_A to W_B expands the double layers around the soil particles and also reduces the electrolyte concentration. The reduced degree of flocculation permits a more orderly arrangement of particles and a higher density... (because)... the increased interparticle repulsion permits the particles to slide past each other into a more oriented and denser bed.

A further increase of water from W_B to W_C results in a further expansion of the double layer and a continued reduction in the net attractive forces between particles. Even though a more orderly arrangement of particles exists at W_C than at W_B , the density of C is lower because the added water

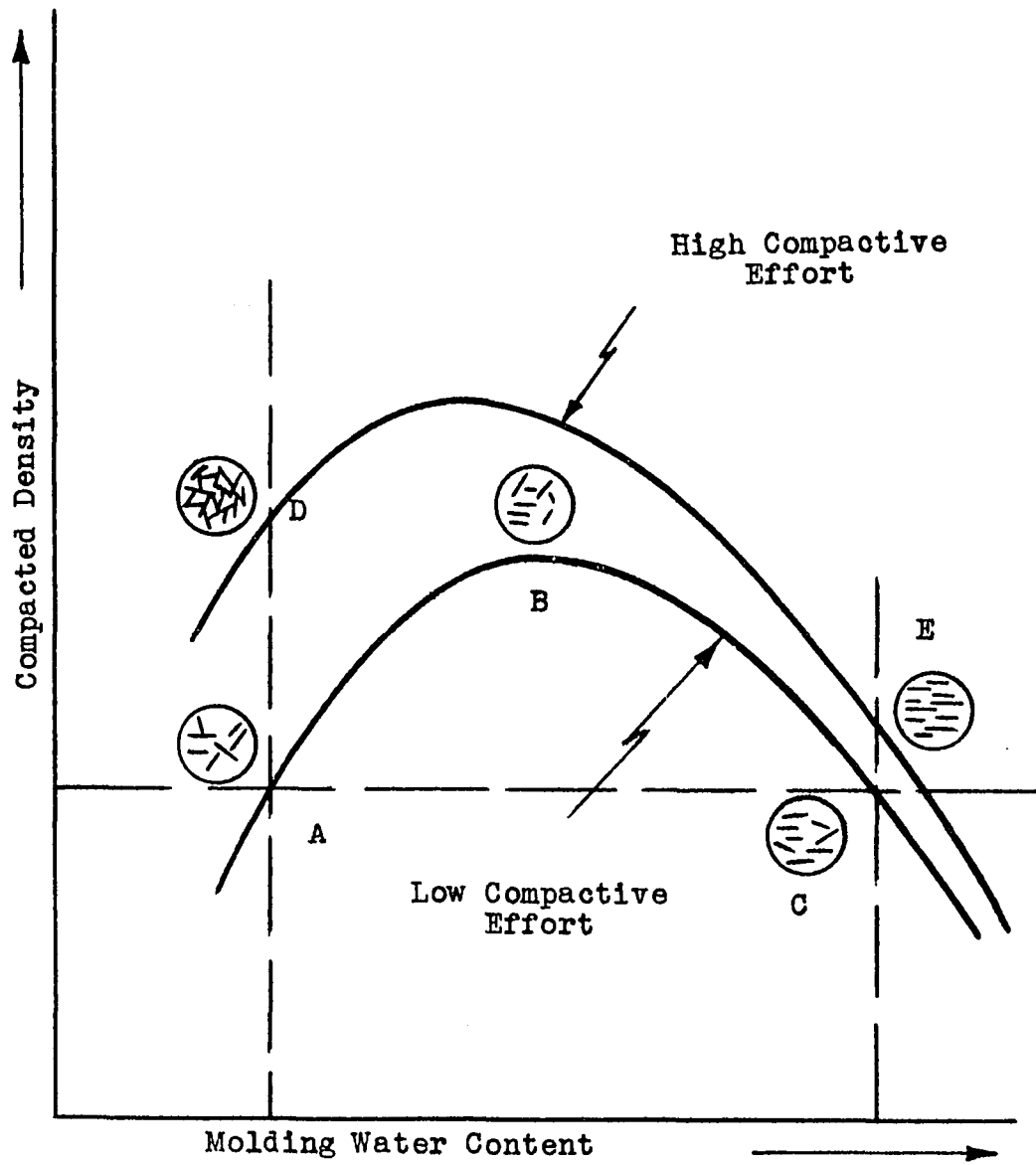


Figure 2

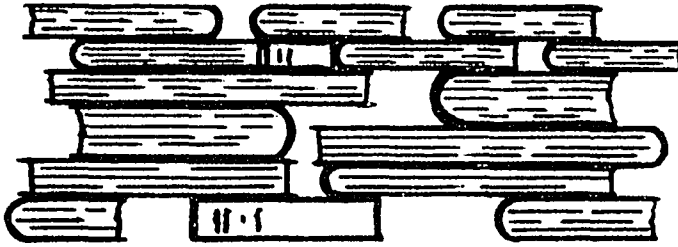
Effect of Compaction
On Clay Fabric (Lambe)

has diluted the concentration of soil particles per volume (there is not a marked decrease in air content from B to C as there was from A to B).

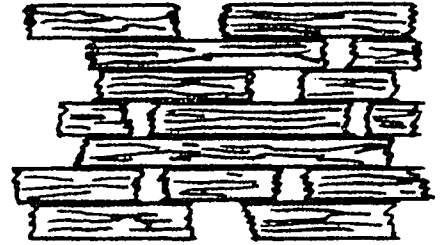
Because of the water deficiency, the water present is subjected to tension as the colloids try to draw water from the outside. Because there is less water at W_A than W_B or W_C , the water deficiency, and thus pore water tension is greater at W_A . (Lambe, 1958a).

Figure 2 also illustrates the effect of compactive effort: the greater the input of work, the closer and more nearly parallel the clay particles. In the present study, it was necessary to choose a randomly-oriented fabric as an initial condition of state. For this reason, all specimens were compacted at a moisture content slightly below optimum in accordance with the concepts of Lambe presented above.

The fundamental notions of soil fabric as presented by Lambe (1953; 1958a) have persisted to this day with few notable exceptions. Kell (1964) in studying the influence of compaction method on the fabric of compacted clay concluded that the term "cardhouse" should not be used synonymously with "randomly-oriented" fabric. He found, through an electron microscope study, that, in compacted kaolinite, edge-to-face contacts between individual particles did not occur, but that the fabric was composed of groups of oriented clay platelets arranged in either an oriented or random fashion. He applied the term "packets" or "books" to these groups. Figure 3, Page 11, shows an analogy between books and packets of clay particles such as were

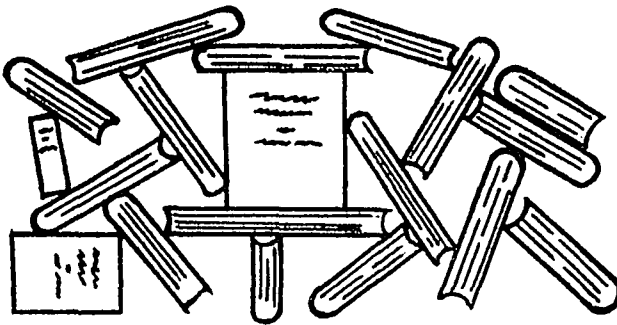


Books

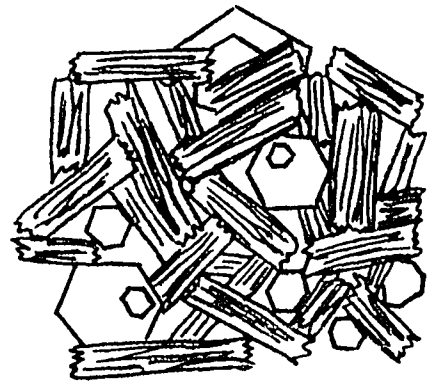


Packets

Oriented



Books



Packets

Random

Figure 3
Book-Clay Packet Analogy (Kell)

observed by Kell.

In the light of the present theory of clay soil fabric, as given above, the current theory on the development of shearing resistance in saturated clay soils and the mechanisms that occur in the shearing process can be better understood.

It has been accepted traditionally that soils possess two fundamentally distinct components of strength: cohesion and friction. This concept finds expression in the Coulomb equation for shear strength and the Mohr failure envelope representation of it. Since these very concepts and the strength theory derived from them are still universally taught and used in practice, it is deemed unnecessary to review them here.

Terzaghi (1925), in introducing the concept of "effective" stress, modified somewhat the Coulomb equation. Further modifications were presented by Hvorslev (1938; 1960) and Rendulic (1937), both students of Terzaghi. The former proposed a relationship between the shear strength, the effective normal stress and the water content of saturated clay. The latter examined the relationship between principal stresses and the water content of cohesive soils. Using the work of Rendulic as a basis, others (Henkel, (1959, 1960); Roscoe, Schofield and Wroth (1958)) developed complex failure theories that introduced such concepts as "stress paths",

"yield surfaces", critical void ratio or "CVR-lines", etc. In all of these studies, the approach made to understand the shear strength properties of cohesive soils relies very heavily upon the results of macroscopic, mechanical tests. The inherent restrictions on the results of such tests prevent them from being used to develop a more fundamental theory of shearing resistance in the shearing process.

That dissatisfaction with the Coulomb equation and related concepts existed very early after its formal application to soils by Terzaghi is evidenced in the attempts of Ter-Stepanian (1936) to examine the shearing process from a micro-structure viewpoint. He found that "chaotically" placed dry mica powder and some undisturbed clays exhibited a trend toward structural orientation and therefore stability after shear. However, physico-chemical considerations were conspicuously absent from his study.

Using the physico-chemical applications to soils as developed earlier by Bolt (1955; 1956), Michaels and Lin (1955) and Rosenqvist (1955; 1957) and as summarized later in the articles of the 1959 Journal of the Soil Mechanics and Foundation Division of ASCE, Vol. 85, SM 2., which was entirely devoted to this topic, Lambe (1958b) examined in detail the nature of shear strength in compacted clays on a micro-structure level. He found that the shear strength of a soil could be considered as composed of a granular-

type strength plus a colloidal-type strength. His investigations revealed that there existed between clay particles certain colloidal forces which, up until that time, had been neglected in studies relating to shear strength. Lambe was able to show that the generally accepted concept of effective stress had to be modified to include the electrical forces of attraction and repulsion. By considering the entire force system, Lambe pointed out that there were four horizontal forces which could act between adjacent colloids and that they were related for dispersed particles as

$$\bar{\sigma} + A - R = 0 \quad (1)$$

and for particles in contact as

$$\bar{\sigma} + A - R = I \quad (2)$$

where

$\bar{\sigma}$ = the externally applied intergranular stress or "effective" stress generally taken as $(\sigma - u)$

where

σ = an externally applied pressure.

u = that part of (σ) carried by the pore water.

A = net electrical attraction (stress).

R = net electrical repulsion (stress).

I = contact pressure that could be due to either steric or geometric interaction.

From this Lambe (1958b) states:

The shear strength of a clay is completely determined by the electrical forces acting between particles, i.e., A, R and I. The electrical forces are thus the primary cause of strength; the four factors,

particle spacing, particle orientation, externally applied stresses and the characteristics of the soil-water system, which determine the electrical forces, are secondary causes of shear strength.

He later summarizes the effects of particle orientation and spacing (fabric) on shear as follows: "For any given void ratio and, therefore, given average particle spacing, the more nearly parallel the particles are, the weaker the soil is". Lambe was cognizant of the fact that the fabric built during compaction would be affected by shear strains which he surmised would align particles. Consequently, he suggested that research be conducted to investigate further correlations of fabric with behavior and to develop a simple test procedure for fabric determination.

Such an investigation was conducted by Seed and Chan (1959a) who attempted to determine the influence of shear in the compaction process on the resulting soil fabric. They concluded that

shear strains apparently tend to produce a dispersed arrangement of soil particles and thus, for soils in which the interparticle forces are not so great that flocculation will occur under all compaction conditions, methods of compaction inducing shear strains produce a greater degree of particle orientation, lower strengths at low strains in undrained tests, greater shrinkage and less swelling than methods of compaction inducing little shear strain. As a consequence of this effect, different methods of compaction tend to produce similar characteristics in samples compacted dry of optimum to any given density and water content but produce different characteristics in samples compacted wet of optimum.

This conclusion is based on the validity of the

Lambe concept of the effect of compaction method and moisture content on soil fabric. That the initial fabric predicted by the Lambe concept was ever realized in the works of Seed and Chan is not evident in their writings. Nor was a quantitative analysis of shear strain and fabric change attempted. From the works of Lambe (1958b), Seed and Chan (1959a, 1959b), Mitchell (1960) and Bishop (1960a, 1960b) it can be shown, however, that

$$S_c = \mu(t) I(t) \quad (3)$$

where S_c = shear strength.

μ = a time-dependent proportionality factor.

I = a time-dependent contact pressure which has been defined above.

From the physical arrangement of any given system of particles the quantity $(A-|R|)$ is, at failure, a function (e_f) of the average distance between particles and the angle between them. However, (e_f) is not a simple function of the void spaces such as is the commonly used "void ratio", but rather it is a function of the fabric of the clay mass. Consequently, equation 3 may be rewritten as

$$S_c = f(\mu, I, e_f, t) \quad (4)$$

Two significant conclusions can be drawn from this expression. The first conclusion is that for infinitesimal values of (t) , i.e. for rapid loading,

$$S_c = f(I, e_f) \quad (5)$$

$$\text{and } I = \bar{\sigma} = \sigma - u \quad (6)$$

whereas for long term effects the value of (I) must include the electrical forces of attraction and repulsion. The second conclusion is that no matter what the loading rate, the shear strength is always a function of (e_f). It is the author's contention that, in this sense, soil fabric is the fundamental component of the physical property termed "shear strength".

In summary, the effect of fabric on the development of shearing resistance in saturated clay soils must be considered for both a dispersed (oriented) and flocculated (unoriented) condition (see Figure 1, Page 7). The mechanism of shearing resistance in an isotropic dispersed clay is largely a function of the particle spacing. In general, any factor which causes a closer particle spacing will alter the distribution of the electrical forces acting between the clay particles. For example, a large externally applied compressive stress may force the parallel-oriented platelets closer together so that the Van der Waals attractive forces would not only increase, but could even become greater than the electrostatic repulsions (Lambe, 1953). In the latter case, the material would exhibit relatively high cohesive shear strength because of the intrinsic attractive forces. In the former case, a greater shear stress would be required to cause a given rate of shear

because of an increase in a viscous-type shearing resistance which exists in the pore fluid as the clay platelets slide over one another.

In isotropic flocculent clays, there is steric and/or geometric interaction between the edges of some particles and the surfaces of other particles which is herein referred to as a "contact". A definite shearing stress is necessary to overcome the attractive force of adhesion created by this edge-to-face arrangement. Consequently, a flocculated clay exhibits a threshold shearing strength. The attainment of this threshold value after application of an increasing shearing stress indicates a condition at which a relatively large portion of the attractive "contacts" in the flocculent fabric are disrupted and, in general, more "contacts" are being broken than made. Throughout this process, particles will tend toward alignment parallel to the plane of shear, and, as a result, the original flocculent fabric will undergo a significant change toward a dispersed fabric. Likewise, strength characteristics will tend toward those of a dispersed clay (at a similar void ratio) although the persistence of some "contacts" will maintain the strength at a higher level than that of a dispersed clay.

It is apparent, therefore, that the mechanism of shear in flocculent clays is quite different from that in dispersed clays. The correlation between these mechanisms

of shearing resistance and the classical concepts of cohesive and frictional components of shear is apparent. The threshold shearing strength corresponds to the cohesive component, and the viscous effect between parallel particles which exists after the cohesion has been destroyed corresponds to the frictional component.

For the anisotropic case, i.e. when the clay fabric is interrupted by a material with larger grains, in whose behavior bulk forces rather than surface forces predominate, shearing stresses in the anisotropic case of a dispersed fabric will cause the particles to interfere with one another during movement. To overcome this interference a threshold shear strength must first be overcome before continuous yielding occurs. In the anisotropic case of a flocculated fabric, the presence of larger grains will cause particle-to-grain "contacts" to occur so that the number of total "contacts" in the anisotropic case will be greater than the number of interparticle "contacts" in the isotropic case. Because the shearing strength depends on the number of contacts, the presence of a wide range of grain sizes will modify the shearing strength of the soil (Scott, 1963).

Scope

From the historical review given above it is apparent that further investigation of the effect of shear strain on soil fabric is necessary before any truly

fundamental theory of shearing resistance can be formulated. The present theory postulates that shearing strains eventually cause parallel alignment of clay particles within the zone of shear (Yong and Warkentin, 1966). Nothing, however, is said of the shearing processes: At what point in that process does the trend toward parallelism begin? Is the transition from randomness to parallelism monotonic or are there reverse trends during the shearing process? What is the relationship between degree of orientation and shear strain?

It is the purpose of this study to investigate the effect of shear strain on soil fabric and by means of x-ray diffraction techniques to qualitatively determine fabric and correlate it to values of shear strain obtained from carefully controlled physical tests. Electron microscopy will be used to verify diffraction data by precisely delineating fabric states.

CHAPTER II

METHODS OF LABORATORY INVESTIGATION

The Cohesive Material Studied

Because it was desirable to use a material of small (less than 2 micron) particle size which exhibited a high degree of crystallinity, which was free from impurities, which did not swell appreciably, and which could be molded easily, a kaolinite clay was chosen as the test material for this research program. The particular kaolinite used, Hydrite UF, is produced and distributed by the Georgia Kaolin Company of Dry Branch, Georgia. The "UF" in the brand name indicates "ultra fine" and is the distinctive feature of this Georgia kaolinite.

The physical and mechanical properties, as determined by the writer, are listed in Appendix A. It may be noted that they compare favorably with those reported by the producer and by others (Martin, 1965; Kell, 1964) working with the same material.

Sample Preparation - Compaction Curve

In order to insure an initially random fabric, theory dictates that specimens be molded dry of optimum moisture (Lambe, 1958). To determine optimum moisture

for Hydrite UF, compaction tests were performed using a modified Harvard miniature compaction apparatus. Individual 120-gram samples of oven-dried kaolinite were mixed with predetermined amounts of distilled water in 4-inch by 8-inch polyethylene bags. Each bag was then manually freed of air, sealed with masking tape, and placed in a high humidity room for approximately 24 hours to allow the sample to cure. At the end of this time each clay sample was removed and compacted in a Harvard miniature compaction mold. The procedure followed was to introduce each sample into the mold in a series of three lifts and to manually tamp each lift 25 times with a 12-ounce rod (the same type as used to perform the saturated surface-dry test on fine aggregate) dropped from a height of approximately two inches. The top of each lift was scarified before addition of the next lift to insure a good bond between lifts. The entire assembly was then capped with a specially machined, tight-fitting plunger through which a statically applied load could be transmitted to the clay sample. The compaction load was applied using a hand-operated, unconfined compression test apparatus at a rate of 7.8 pounds per second until the load that induced a stress of 500 lbs/sq in was reached. This load was held for one minute. The moisture-density results of the compaction tests are presented in Figure 4, Page 23, as the static compaction curve for the kaolinite. A compactive pressure of 500 lbs/sq in

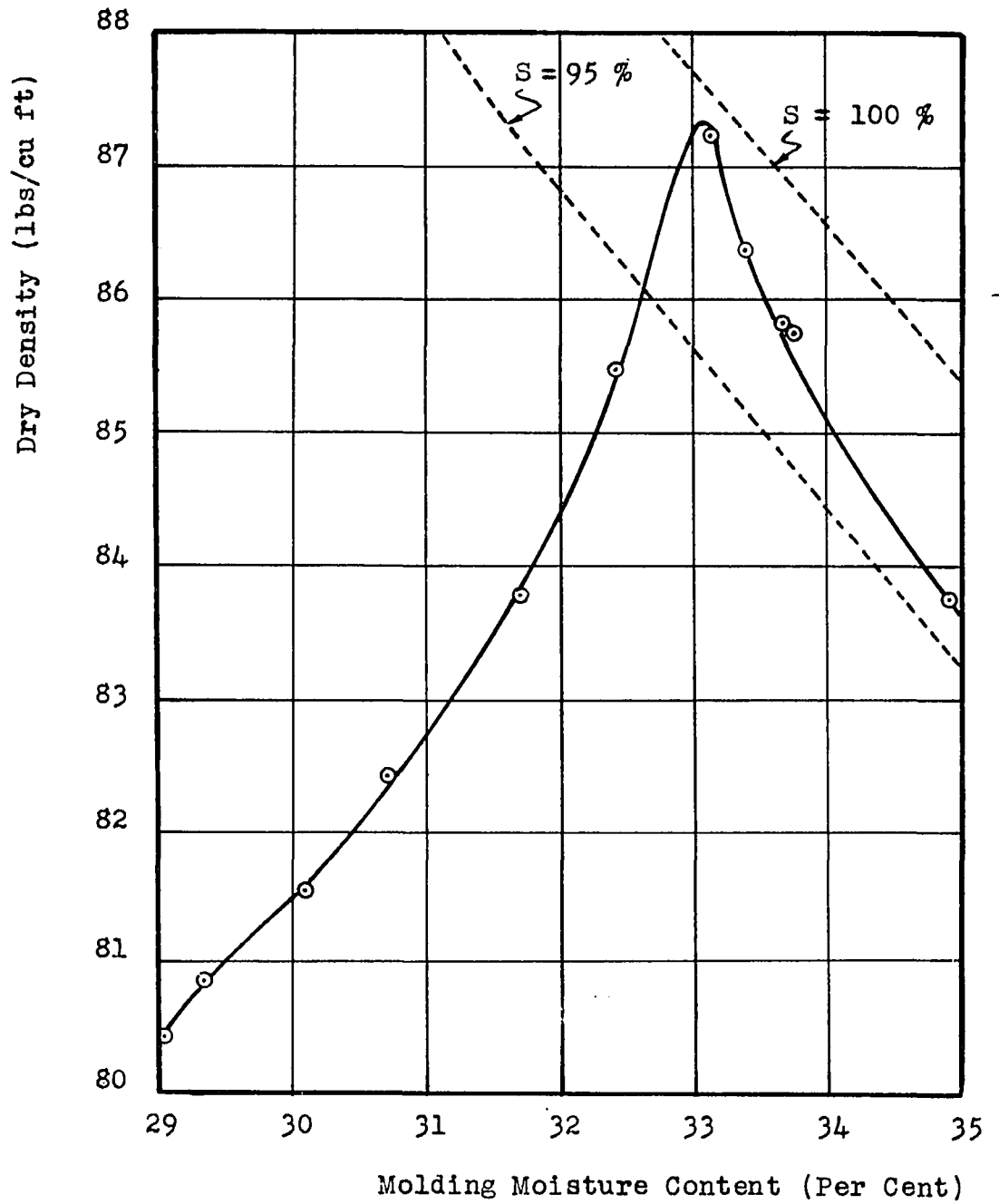


Figure 4

Static Compaction Curve for Hydrite UF
at a Compactive Effort of 500 lbs/sq in

was used in order to obtain a condition as close to 100 per cent saturation as possible without significantly affecting the desired randomly-oriented fabric.

Sample Preparation - Direct Shear

a) Compaction:

With optimum moisture having been determined as 33.1 per cent for a 500 lbs/sq in compactive effort, the molding moisture content for the direct shear samples was arbitrarily chosen as 32.0 per cent, \pm 0.6 per cent. Molding samples at this "dry of optimum" moisture should assure the desired randomly-oriented fabric for the initial condition.

In order to hold the molding moisture content within the specified tolerance, 5-kilogram batches of kaolinite were oven dried for at least 24 hours at 100°C. From one such large batch an individual 1,280-gram sample was chosen and placed in a 16-inch by 24-inch polyethylene bag. To this, 410 grams of distilled water were added carefully with a minimum of splashing.

After most of the air had been manually squeezed from the bag, the open end was carefully folded over, tied tightly with a piece of twine, and sealed with a strip of masking tape. The contents of the bag were then quickly kneaded by hand until no free moisture was visible. The immediate consequence was the formation of clay balls

ranging in size from 1/8-inch to 3/4-inch, a condition indicative of areas of locally high moisture content. This undesirable condition was remedied by striking the balls with a rubber mallet until they were sufficiently broken down to allow a more even distribution of moisture throughout the sample. Since the entire operation was performed on sealed samples, no significant loss of moisture occurred. Each sealed sample was then doubly wrapped in 9-inch by 18-inch polyethylene bags, again sealed with tape, and finally placed in a high humidity room to cure for not less than one week. Upon removal from the high humidity room each sample was stripped of the two outer polyethylene bags and reworked with the rubber mallet for about 15 minutes. The inner seal was then broken and the clay carefully introduced into a four-inch-diameter tapered standard compaction mold in a series of three lifts. Each lift was manually tamped 10 times with a specially machined, 3,555-gram aluminum plunger dropped from a height of approximately three inches. The contents of each bag, when introduced in this way, just filled the compaction mold to the top of the collar. The entire assembly was then placed in a 30,000 pound compression machine. In order to duplicate the loading conditions used in the determination of the compaction curve, the compression rate was set at 80 pounds per second until a total load of 6,280 pounds was reached. The load was held automatically at that value for one minute. A static load of 6,280 pounds induced a stress of 500 lbs/sq in

on the sample in the compaction mold. Each sample was then weighed to check the wet density against the value computed from the 84.4 lbs/cu ft dry density obtained from the compaction curve for a molding moisture content of 32 per cent. All the samples checked to within ± 1.5 lbs/cu ft which, in view of the sharp drop of the compaction curve on the dry side of optimum moisture, was considered satisfactory. A sample ejector was used to remove the kaolinite from the compaction mold.

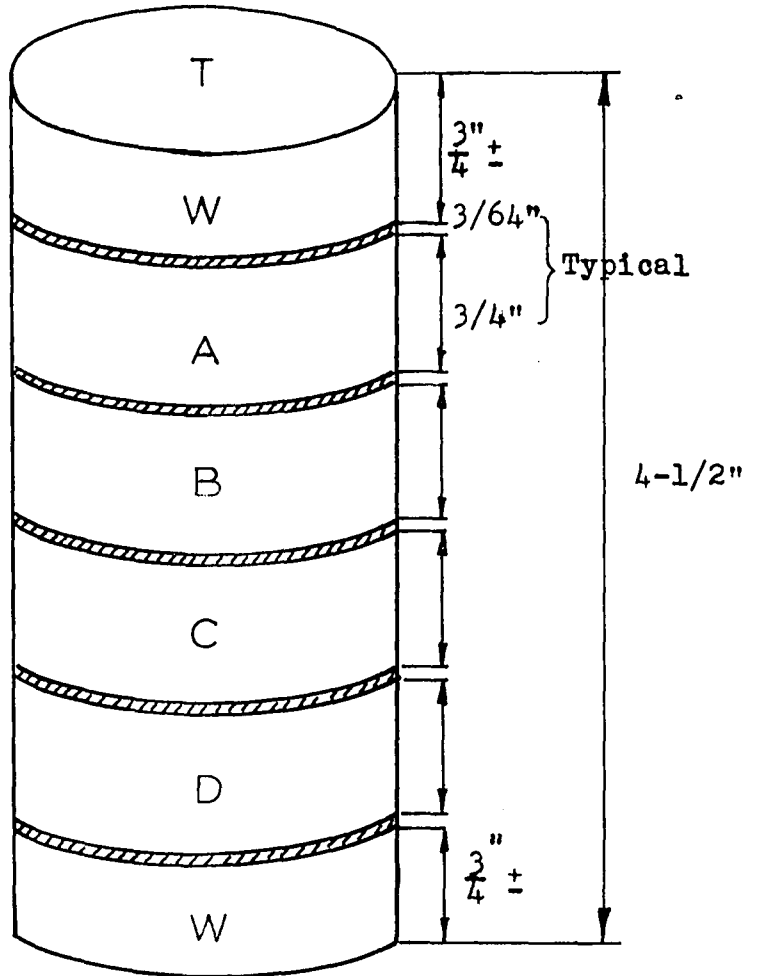
b) Shear Samples:

Upon removal from the compaction mold the sample was immediately trimmed lengthwise with a knife to approximately 2.5 inches in diameter. A portion of this rough trim was taken for the moisture content determination. A motorized soil lathe was used to further trim the sample to an exact diameter of 2.0 inches. Care was exercised to keep the trimmer in such a position that the cut would be uniform down the length of the sample and that no "biting" would occur. Care was also taken to keep the sample oriented with respect to the compaction load, i.e., the surface that had been in contact with the compaction plunger was marked "T" while the surface that had been at the bottom of the compaction mold was marked "B". This was done to minimize the effect of a non-uniform stress distribution during compaction, i.e., the shear samples for a given per cent of failure strain would all be cut from the same 4.5-inch length,

however, for each per cent of failure strain, the sample for a given normal load would always be taken from the same relative position within the respective 4.5-inch sample. Figure 5, Page 28, illustrates the procedure. A saw and miter box were used to cut four individual shear samples from the 4.5-inch gross sample. Each shear sample was 2 inches in diameter and 0.75 inches thick. The top and bottom 0.75 inches of the gross sample were discarded since they had been disturbed by the lathe's gripping teeth. Having been appropriately marked to define their position, the shear samples were then individually wrapped and sealed in two plastic bags until ready for testing in the direct shear apparatus. In order to keep moisture loss at a minimum and in order to eliminate the influence of any thixotropic effects, the shear tests were performed within one hour of the cutting of the shear samples.

Direct Shear Tests

The direct shear test was chosen in preference to the triaxial test because of the necessity to know the approximate position of the shear zone at any time during the shearing process. The direct shear test, by imposing the shearing plane, assured this requirement. Depending upon the normal load, a shear sample was chosen in accordance with the convention shown in Figure 5. The sample was removed from the plastic bags and quickly placed in the 2-inch diameter shear box of the direct shear apparatus,



Section *	Normal Load (kg/sq cm)
A	0.4
B	0.8
C	1.2
D	1.6
W	Waste

* All 3/4-inch samples taken from a given, common, 4-1/2-inch sample are tested to the same per cent of failure strain.

Figure 5

Procedure For Cutting Shear Samples

U.S.B.P.R. design. Moist cotton had been carefully placed around the shear box so that the specimen would retain moisture until the actual shear test began. The normal load was then applied through a compact lever system and a plot made of consolidation versus square root of time to determine the completion of primary consolidation. Due to the comparatively high static compaction load, the applied normal loads did not appreciably effect further consolidation of the shear samples over a ten-minute period of time.

A distinctive feature of the direct shear device used was that the shearing loads were applied through an electrically driven, variable speed transmission controlled by a micrometer dial. This made it possible to accurately set the loading rate at 0.0125 inches per minute for all the direct shear tests conducted. The slow rate of shear allowed adequate time for virtually complete drainage of the sample to take place during the shearing process so that the effect of induced pore-water pressures could be neglected.

In the first series of tests the shearing load was applied until complete fracture of the sample took place. A series consisted of tests performed with normal loads of 0.4, 0.8, 1.2 and 1.6 kg/sq cm. During this series, readings were taken of the proving-ring dial (load) and the shear dial (horizontal displacement) every 15 seconds until the load reading began to decrease. A vertical displacement reading was also taken at the beginning and end of each test

to determine whether the sample had contracted or expanded vertically during shear. From the data obtained in this "failure series" of tests, shear-stress versus shear-strain diagrams were plotted for the various normal loads as shown in Figure 6, Page 31. Maximum shear stress was chosen as the failure criterion and the strain at that stress was taken as the failure strain. For each condition of normal load, arbitrarily chosen percentages (75, 50, 25) of this failure strain were computed and the associated value of stress obtained from the stress-strain curve. These values of stress and strain were converted respectively into the corresponding proving-ring dial and horizontal-displacement dial readings. Another series of shear tests was then performed on a new set of samples. In this series the horizontal displacement was brought to a predetermined value depending upon the percentage of failure strain desired. The proving-ring dial was also read to check the reproducibility of the original failure stress-strain curve. Reproducibility was excellent in most cases and, even in the worst case, the error was less than 10 per cent. Immediately upon completion of the shear test, the sample was removed from the shear box, marked on front and top, and placed into a pan of melted Carbowax 6000, a product of the Union Carbide Company. Carbowax 6000 is a water soluble wax and, because of this, is ideally suited to replace the moisture in the sample by diffusion and thereby not disturb the fabric (Mitchell, 1956). The pan containing the strained samples of a given test

to determine whether the sample had contracted or expanded vertically during shear. From the data obtained in this "failure series" of tests, shear-stress versus shear-strain diagrams were plotted for the various normal loads as shown in Figure 6, Page 31. Maximum shear stress was chosen as the failure criterion and the strain at that stress was taken as the failure strain. For each condition of normal load, arbitrarily chosen percentages (75, 50, 25) of this failure strain were computed and the associated value of stress obtained from the stress-strain curve. These values of stress and strain were converted respectively into the corresponding proving-ring dial and horizontal-displacement dial readings. Another series of shear tests was then performed on a new set of samples. In this series the horizontal displacement was brought to a predetermined value depending upon the percentage of failure strain desired. The proving-ring dial was also read to check the reproducibility of the original failure stress-strain curve. Reproducibility was excellent in most cases and, even in the worst case, the error was less than 10 per cent. Immediately upon completion of the shear test, the sample was removed from the shear box, marked on front and top, and placed into a pan of melted Carbowax 6000, a product of the Union Carbide Company. Carbowax 6000 is a water soluble wax and, because of this, is ideally suited to replace the moisture in the sample by diffusion and thereby not disturb the fabric (Mitchell, 1956). The pan containing the strained samples of a given test

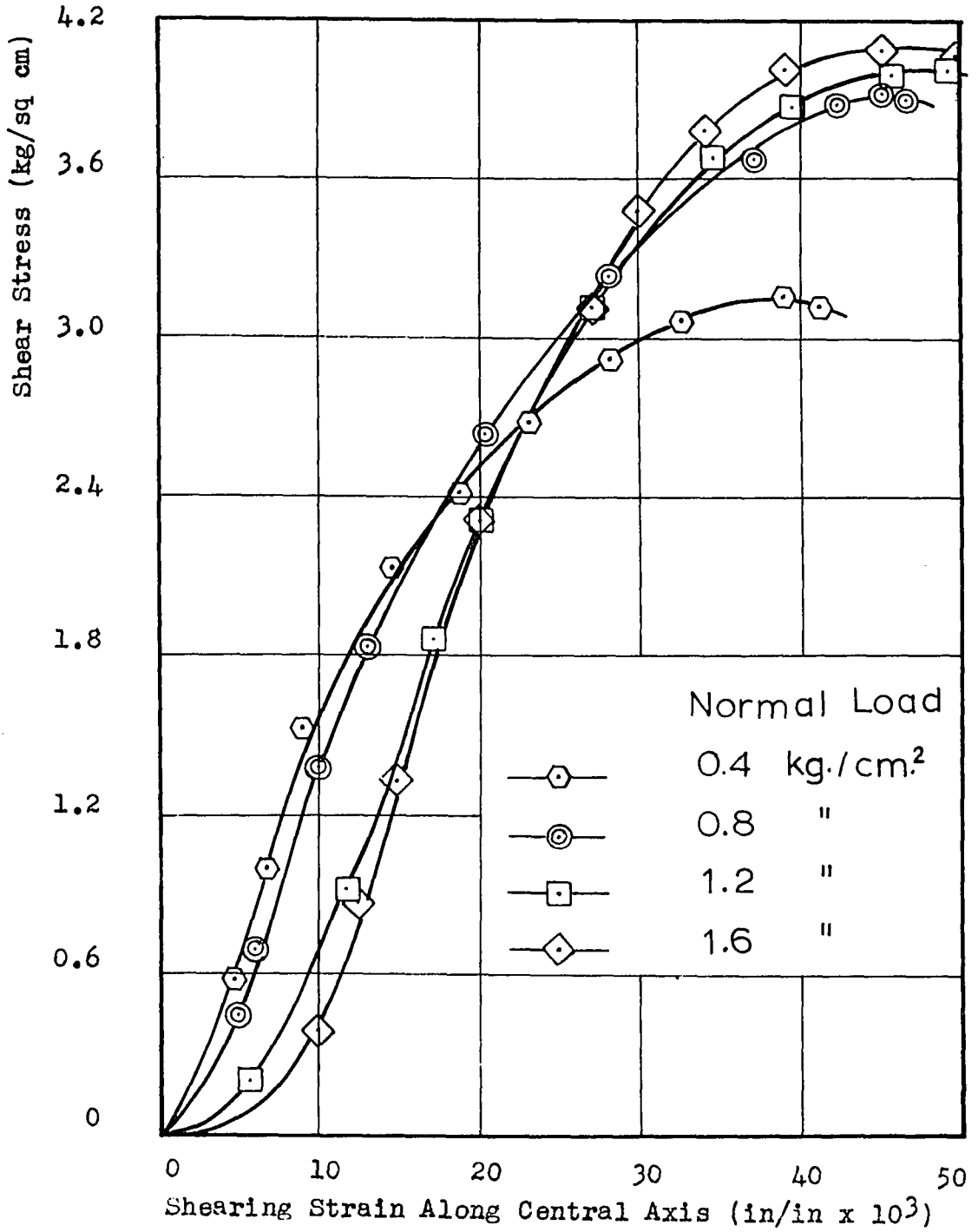


Figure 6

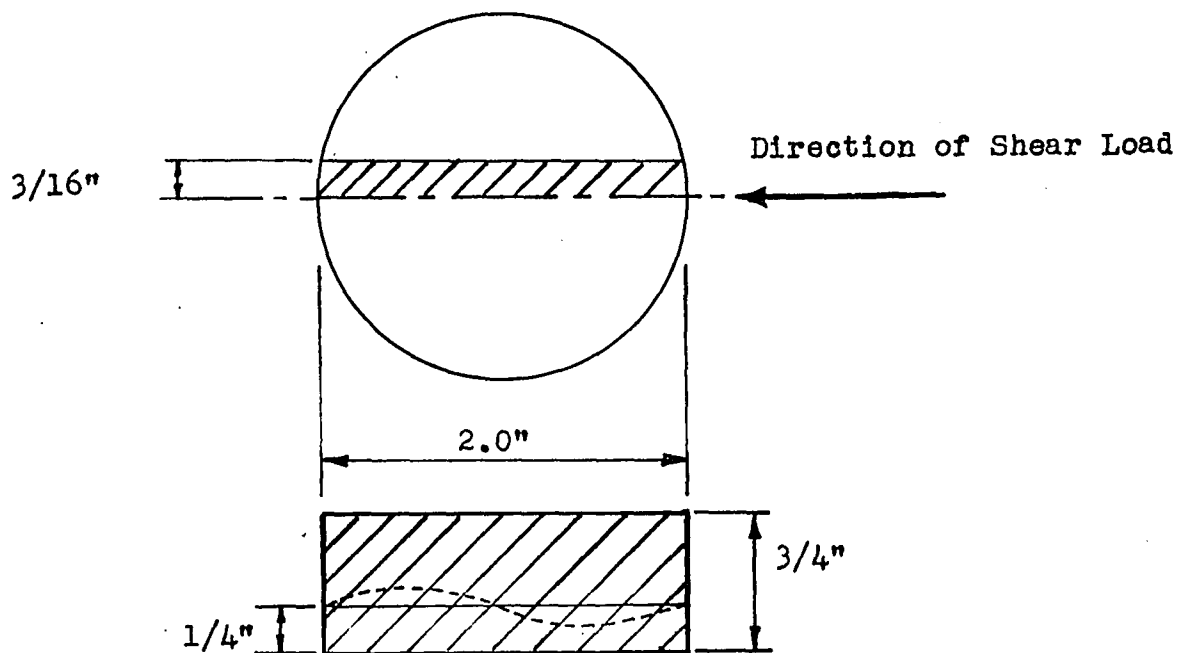
Shear Stress Versus Nominal Shearing Strain
For Various Normal Loads

series was kept in a constant-temperature oven at 65°C for a minimum of 12 days. The Carbowax was periodically changed so that the moisture replacement could take place efficiently. At the end of the soaking period the samples were removed from the wax and allowed to harden for approximately one week until they were rock-like at about talc hardness. Each shear sample was now ready for cutting into two x-ray diffraction specimens.

X-ray Diffraction Study

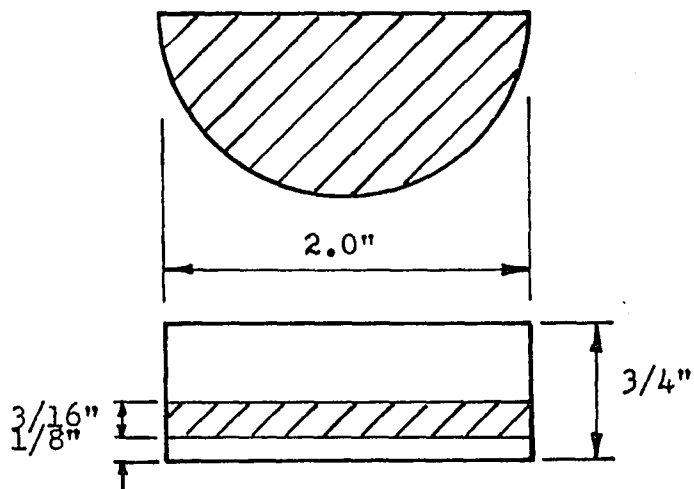
a) Specimen Preparation:

To prepare a vertical specimen for diffraction the Carbowax-impregnated sample was bisected along the diameter parallel to the axis of the applied shearing load. On the right half of the bisected sample another cut was made 3/16-inch away from and parallel to the center plane as shown in Figure 7(a), Page 33. The rough, 3/16-inch thick rectangular section was then held on a motorized sander until the center face was smooth to the touch. After the gross irregularities due to sawing had been removed in this way, the sanded surface was wet polished in kerosene on number 600 carborundum paper. Special care was taken during the wet polishing to use uni-directional strokes and only slight finger pressure. The specimen was considered suitable for x-ray diffraction when, under a light microscope at 60X magnification, it could be determined that the treated surface was flat and free from



(a)

Vertical Specimen



(b)

Horizontal Specimen

Figure 7

Procedure For Cutting X-ray Diffraction Specimens

holes and excessive cracks. That the above procedure does not adversely affect the fabric has been amply demonstrated by R.T. Martin (1965).

Before preparation of a horizontal specimen could begin, the approximate extent of the shear zone had to be known. It was decided to measure the failure zones of the four fractured samples from the profile afforded by the vertical specimens. An average value of 3/16-inch was used as the thickness for all horizontal specimens except the failure specimens for which the actual zone thicknesses were used. Although the failure zones were irregular in shape because of density gradients formed during the shearing process (see Figure 7(a), Page 33, profile view), the horizontal plane through the center of the shear zone was taken as that imposed by the shear box itself. The horizontal specimens were cut to include this plane (refer to Figure 7(b)). The surface-finishing treatment was the same as that used for the vertical specimens described above.

Immediately following preparation, the specimens were placed in an appropriately identified plastic Petri dish and stored in a chemical desiccator until ready for the x-ray diffractometer. Petri dishes containing vertical specimens were marked "NVM" while those containing horizontal specimens were marked "NHM" where in both cases:

N = the per cent of failure shear-strain to which the sample had been subjected.

M = the magnitude of the normal load in kg/sq cm.

This notation is used throughout to properly identify specimens under discussion.

b) X-ray Diffraction Equipment:

A late model General Electric XRD-5 x-ray diffractometer having a digital printer was used for the entire diffraction study. The x-ray beam consisted of copper radiation produced at 35 kv and 23 ma. The emitted beam was modified by a 1° beam slit before impinging upon the goniometer-mounted specimen. The diffracted beam then passed through a medium resolution collimator, a 0.1° detector slit and a nickel filter before reaching the detector tube, an SPG-6 xenon-filled proportional counter tube. Only peak counts were desired; therefore, the goniometer was moved manually from peak to peak in the manner described below.

c) X-ray Diffraction Technique:

From a comparison of the diffraction traces of powdered kaolinite, Carbowax 6000 and Carbowax-impregnated kaolinite it was decided that the best peaks to use for this study would be the (002) peak and the (020) peak. The former was preferred over the (001) peak because the (002) peak is closer in the 2θ diffractometer angle to the (020) peak. Both the (002) peak and the (020) peak were sufficiently well

defined so that the goniometer could be accurately placed at the desired peak by the following procedure:

1) To obtain the peak-count at the (020) peak, the goniometer was manually advanced from a 2θ angle of 19.40° at a rate of approximately 0.5° per minute.

2) When the diffraction trace reached a maximum, the rate of advance of the goniometer was decreased until the diffractometer trace could be noted to just begin to fall off. Mental track was kept of the amount of advancement that took place at this reduced rate and the goniometer was reversed half this distance and locked into place.

3) A series of 10 random counts, each taken over a 10-second scan time, was automatically recorded at this setting.

4) The goniometer was manually returned to $19.40^\circ 2\theta$ and the above steps repeated.

5) To obtain the peak-count at the (002) peak, the goniometer was preset at $24.40^\circ 2\theta$ and then manually advanced at a rate of approximately 0.5° per minute.

6) The procedure in steps 2) and 3) was also followed to locate the (002) peak accurately and to record a series of peak counts.

7) The above two steps were repeated.

8) The specimen was rotated 180° in the specimen holder and steps 5) and 6) repeated twice.

9) The goniometer was then manually returned to a

2θ angle of 19.40° and steps 1) through 3) repeated twice.

Repetition was considered necessary in order to offset the influence of background radiation on the peak-locating procedure described above. Rotation of the specimen was also considered necessary since any significant difference in the counts would indicate a poor preparatory polishing procedure. Fortunately, no great differences were noted. Nevertheless, whenever even slight differences in the trace were visually observed, an additional series of counts was taken and included as part of the average count for both peaks of the given specimen. All of the diffraction work was performed at approximately the same time each day so that the effect of local electrical disturbances on the background radiation count was minimized. The actual background count for each specimen was determined from the diffraction traces. At the 2θ values investigated the background count did not vary appreciably from day to day either for the same impregnated specimen or between different impregnated specimens or between impregnated specimens and non-impregnated specimens.

The peak-count data obtained on paper tape from the digital printer were transferred to standard 8-word IBM cards. A Fortran program was written to compute the mean peak count at both peaks, the average orientation index, and the standard deviation of the data from the mean for both the (020) peak and the (002) peak for each specimen. By definition, the

orientation index is the ratio of the average peak-count at the (020) peak minus the background count at that peak to the average peak-count at the (002) peak less its background count.

$$O. I. = \frac{\text{Average peak-count at (020)} - \text{Background at (020)}}{\text{Average peak-count at (002)} - \text{Background at (002)}} \quad (7)$$

Electron Microscope Study

In order to substantiate the conclusions drawn from the results of the diffraction data by actually observing the fabric changes in the sheared specimens, and in order to quantitatively describe the size of the shear zone, an electron microscope study was undertaken. Because the purpose of this study was to investigate fabric-related changes only, it was decided that surface-replica microscopy rather than transmission microscopy would be most desirable. Two-stage replication was chosen because it was thought best to save the diffraction specimens should there be any need for reruns subsequent to the microscope study. The details of the study follow:

a) Replica Preparation:

Due to time limitations it was impossible to conduct an electron microscope investigation of all the x-ray diffraction specimens. Consequently the 1.2 kg/sq cm series was chosen as most representative of the entire group and

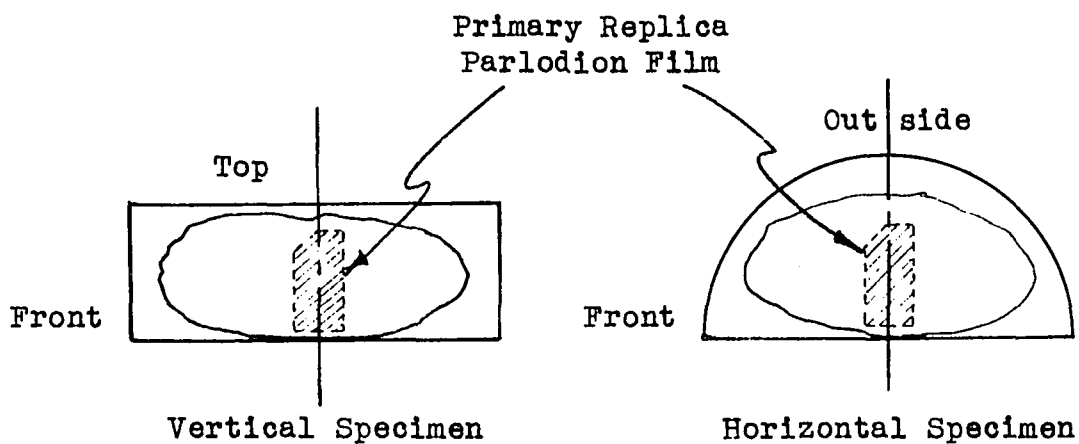
replicas were made of each diffraction specimen of this series in both vertical and horizontal orientations. It must be remembered that the diffraction specimens were impregnated with Carbowax and, therefore, were unsuitable for direct replication. Special treatments were conceived and used to prepare the surface of the sheared specimens for replication. All chemicals used in these preparatory treatments and throughout the electron microscope study were American Chemical Society reagent grade.

It was found that 100 drops of ethylene dichloride applied approximately 1/8-inch from the surface which was tilted at an angle of 30° would be adequate to etch the surface of a diffraction specimen deep enough for replication of surface detail and fabric and not deep enough to destroy the specimen. A tilt of 30° was sufficient to allow the ethylene dichloride to run and therefore etch the length of the specimen, yet not steep enough to cause "scour" in the surface and thereby seriously alter the fabric of the strained specimen.

Following the ethylene dichloride treatment the etched specimen was placed in a dust-free container and subjected to vacuum desiccation for at least 24 hours. After removal of the specimen from the desiccator, a 4 per cent solution of parlodion in amyl acetate was applied quickly to the etched surface. The solution was allowed to air-dry at least

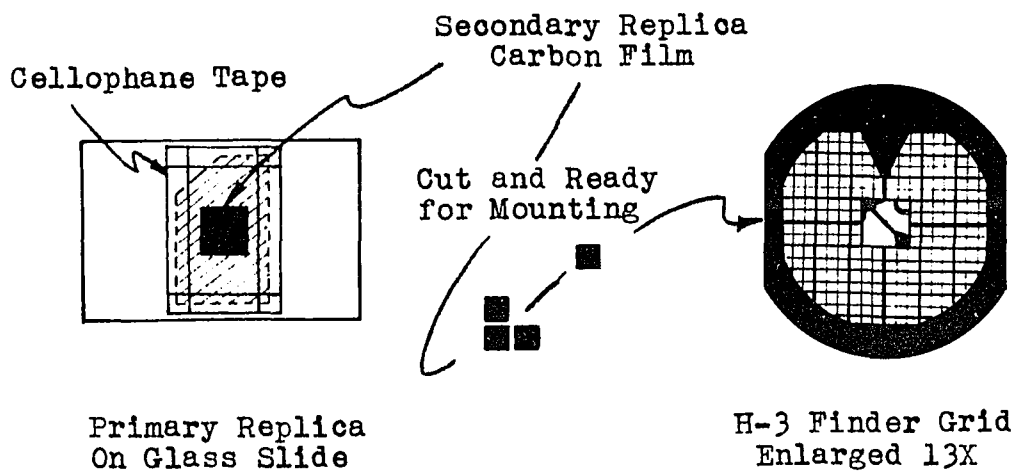
24 hours. The very thin parlodian film formed at the end of this time served as the first stage or primary replica. The film was carefully cut with a razor blade in the manner shown in Figure 8(a), Page 41, and shaved off the surface of the specimen. By cutting and removing the film in this way a dual purpose was served: first, the orientation of the primary replica relative to the top and front of the specimen was preserved; and, second, the removal of material with the primary replica in the shaving process did not materially disturb the fabric so that, if necessary, the x-ray diffraction specimen could be kerosene wet-polished and reused.

Upon removal from the specimen surface, the parlodian film was placed in an ultrasonic cleaner. A small amount of water was added and the film, submerged in the water, was then subjected to ultrasonic cleaning for approximately five minutes. This treatment removed many of the large pieces of kaolinite embedded in the film. To effect the removal of Carbowax from its surface, the film was subjected to three separate one-hour baths in a fresh solution of ethylene dichloride. To complete the dissolution of kaolinite from its surface, the film was finally cleaned in concentrated hydrofluoric acid. Three four-hour cleansings in the acid were alternated with ten-minute water washes. The film was then placed in the ultrasonic cleaner for one minute as the final treatment before replication. After



(a)

Primary Replication



(b)

Secondary Replication

Figure 8

Primary and Secondary Replication
And Mounting Procedure

this treatment the film was allowed to air-dry in a dust-free container. The process described above yielded a replicating surface clean of both carbowax and kaolinite.

After drying, the primary replica was mounted on a glass slide, impression side up. A thin lead-foil mask having a square opening was used to isolate a selected surface of the film for replication. The entire assembly was then placed in a thin-film vacuum evaporator. After low-angle platinum-palladium shadowing, the carbon second-stage replica was evaporated onto the film by the Bradley (1954) method. Upon removal from the evaporator the replicated portion of the film was cut carefully into 2 mm squares for mounting on type H-3 finder grids (a product of Graticules Limited, London, England). This procedure is shown in Figure 8(b), Page 41. The use of finder grids enabled the orientation of the specimen relative to the applied shear to be determined immediately while viewing it in the electron microscope. The mounted two-stage replicas were then placed on a stainless steel mesh bridge and the parlodion primary replica dissolved by bathing for one hour in three separate baths of fresh acetone. By not allowing the level of the acetone to exceed the height of the bridge, the grids were kept from floating in the acetone and the danger of the second-stage carbon replica being floated free of the grid was avoided. If this were to happen, orientation would be lost. At the end of this treatment

only the second-stage carbon replica mounted in proper orientation on the finder grid remained. It was now ready for viewing in the electron microscope.

b) The Electron Microscope:

All replicas were viewed in an Hitachi Electron Microscope Model HS-7 having a resolution of 15 Angstroms and an electron optical magnification of between 1,500X and 50,000X. An internal camera chamber allowed the taking of electron micrographs on 3-1/4 x 4-inch glass plates.

c) The Electron Microscope Study:

There were four replicas made of each polished surface in both the horizontal and vertical orientation. For the normal load of 1.2 kg/sq cm there were five distinct conditions of strain (0, 25, 50, 75, and 100 per cent). Therefore, a total of forty replicas were viewed under the electron microscope. All viewing was done at a magnification of 5000X. The quality of the replication varied so that, in general, only two or three replicas of each set of four were suitable for detailed study. The major part of the viewing effort was concentrated upon the vertical specimens because they contained the shear zone in profile. Whenever a distinctive fabric feature was noted on either a horizontal or vertical specimen, an electron micrograph was taken.

After the initial viewing of both horizontal and vertical specimens, an attempt was made to measure the extent of the shear zone. Using vertical specimens only, this was accomplished in the following manner: at a given magnification one side of the 8 cm square field on the microscope view screen corresponded to a certain magnified length. By using this side as a unit of measurement, the length of one opening and one grid bar of the H-3 finder grid could be laid off and quite accurately determined. The fabric changes of the specimen being viewed could then be noted from grid opening to grid opening and the extent of the shear zone computed by simply adding up the number of grid openings and grid bars and multiplying by the magnified size of each. In general, three or four such determinations were made for each per cent strain and an average taken for the shear zone extent reported.

CHAPTER III

PRESENTATION AND DISCUSSION OF RESULTS

General

The study is composed of three phases: a preliminary investigation of the physical properties of the kaolinite material itself, in particular its shearing properties; the x-ray diffraction study; and the electron microscope study. Each phase has its own singular results as well as results that can be correlated to the other phases. The presentation and discussion will be in the order as listed above which is also the order in which the phases were performed.

Preliminary Investigations

The moisture-density and shear stress-strain relationships of Hydrite UF were of major interest in this phase of the study. Other physical properties were investigated and the results appear in Table 1 of Appendix A, Page 78.

The Moisture-Density Relationship

By carefully following the shear-sample molding procedure described in Chapter II, the moisture content of all the samples prepared for shearing was kept to within

± 0.6 per cent of the chosen molding moisture content of 32.0 per cent. After compaction the wet density was determined; the dry density was computed and checked against values obtained from the compaction curve presented as Figure 4, Page 23. The results, listed in Table 2 of Appendix A, Page 78, agree to within ± 1.0 per cent of the values predicted by the moisture-density relationship of Figure 4 and were considered to be satisfactory.

The Shear Stress-Strain Relationships

The stress-strain curves for various normal loads (Figure 6, Page 31) were used according to the manner described in Chapter II. The curves reflect typical characteristics of partially saturated cohesive soils tested in a direct shear device at a very slow rate of shear. With increase in normal load both the peak shearing stress and the slope of the stress-strain curve increase.

There are, however, some non-characteristic features. All curves are non-linear at low shearing stresses and strains. Non-linearity may be attributed to adjustments of the mechanical components of the direct shear device at the initiation of each test. By defining failure strain as the strain associated with the peak shearing stress and by working with percentages of the failure strain, the effect of the initial non-linearity was minimized. As a check, for each sample strained to a given per cent of failure strain,

the reading of the proving-ring dial gage (shear stress gage) was compared to that of the "failure" test at the same strain. The difference was negligible in most cases. The per cent error in even the worst cases was always less than 10 per cent. There is no well defined relationship in the curves of Figure 6 between peak stress and the corresponding strain, as exists for granular soils. For granular materials there is a definite decrease in the strain corresponding to peak stress with increase in normal load. This problem, however, is outside the scope of this study.

For this study, the stress strain curves of Figure 6 adequately define the values needed for an examination of the effect of shear strain on fabric.

The X-ray Diffraction Study

In order to determine the orientation index (defined in Chapter II, page 38) at the limit conditions three ideal randomly-oriented powder specimens and three parallel-oriented slide specimens were x-rayed and an average used. The method of preparation for the former is described by Martin (1965) and for the latter by Warshaw and Roy (1961). The peak-count data for these specimens and for all of the Carbowax-impregnated specimens were processed on an IBM 1401-7072 digital computer and the following results obtained: the mean peak-counts for both the (020) and (002) peaks; the average orientation index; and the standard deviation of the data

from the mean for both peaks. The average orientation indices are listed in Table 3, page 49, and the remainder of the pertinent computed results appear in Appendix B, page 80. Figures 9 and 10 present in graphical form the results shown in Table 3. It is interesting to note the following features from the curves in Figures 9 and 10:

- 1) The fabric of the horizontal specimens is more dispersed in every case than that of the vertical specimens, as shown by the differences in the orientation index. This is an expected result because horizontal specimens were taken from a plane normal to the direction of the applied compaction load.

- 2) The initial condition of the fabrics of the impregnated specimens, as represented by the orientation index of the IC-V0.0 specimen can be considered random because the orientation index of the IC-V0.0 specimen is close in value to that of the control ideal randomly-oriented specimen. The orientation index of the IC-H0.0 specimen is, as expected, lower indicating a more dispersed fabric. Because the orientation index is not nearly as close to the value of the control parallel-oriented specimen as the IC-V0.0 value is to the control ideal randomly-oriented value, it would be a gross error to say that the IC-H0.0 specimen is indicative of a dispersed fabric. Although only one specimen was used to determine the initial condition, it is safe to conclude

TABLE 3

Average Orientation Indices For Both Carbowax-impregnated
Test Specimens And Non-impregnated Control Specimens

Specimen	Average Orientation Index
100VO.4	0.46
75VO.4	0.47
50VO.4	_____*
25VO.4	0.39
100HO.4	0.21
75HO.4	0.33
50HO.4	_____*
25HO.4	0.30
100VO.8	0.50
75VO.8	0.48
50VO.8	0.45
25VO.8	0.40
100HO.8	0.29
75HO.8	0.28
50HO.8	0.25
25HO.8	0.26

* Data missing due to error in cutting procedure.

TABLE 3--Continued

Specimen	Average Orientation Index
100V1.2	0.37
75V1.2	0.46
50V1.2	0.56
25V1.2	0.50
100H1.2	0.25
75H1.2	0.20
50H1.2	0.20
25H1.2	0.24
100V1.6	0.48
75V1.6	0.48
50V1.6	0.50
25V1.6	0.45
100H1.6	0.27
75H1.6	0.22
50H1.6	0.21
25H1.6	0.21
IC-V0.0	0.48
IC-H0.0	0.30
Ideal Randomly-Oriented	0.68
Parallel Oriented	0.03

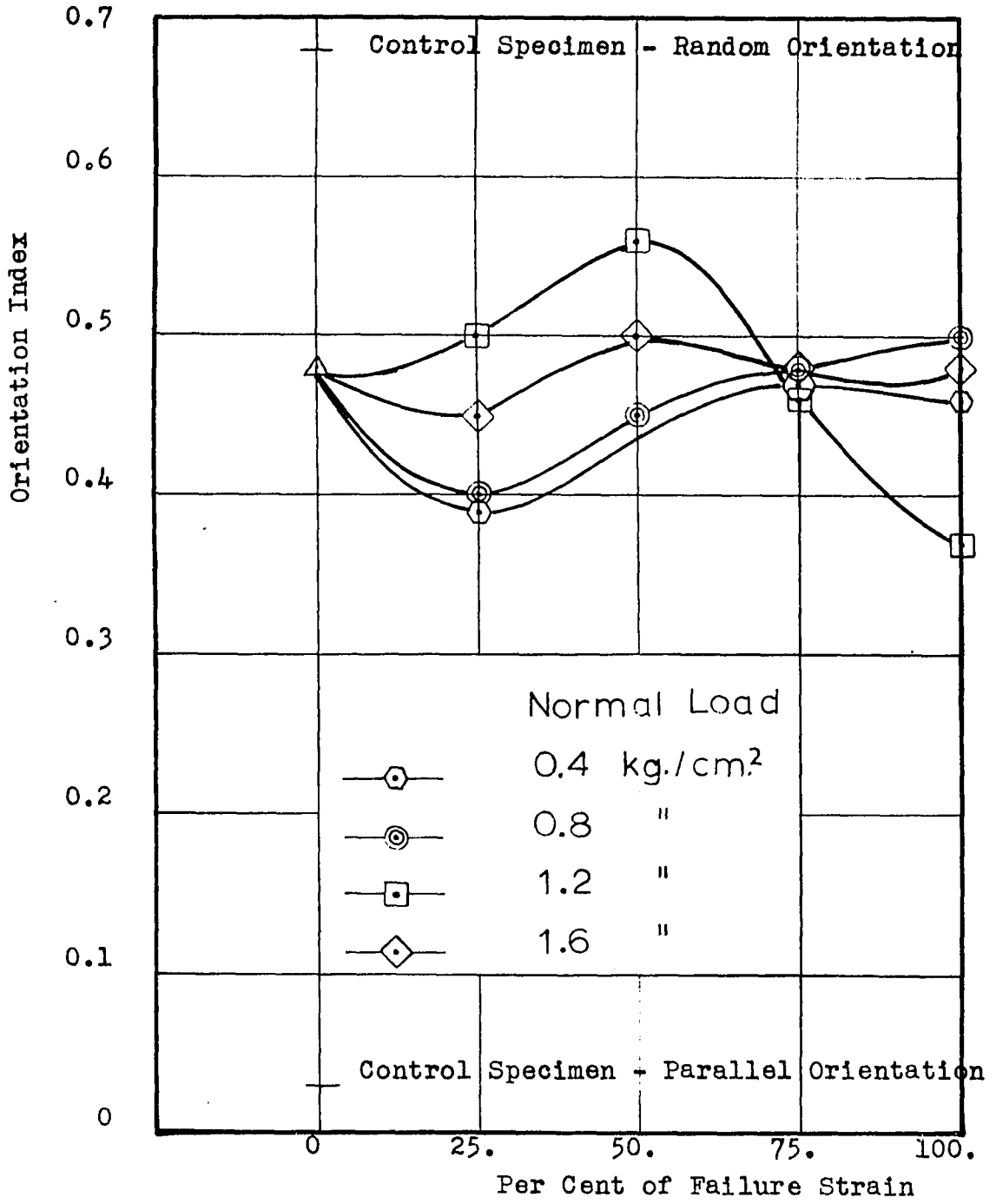


Figure 9
 Variation of Orientation Index With
 Per Cent of Failure Strain - Vertical Specimens

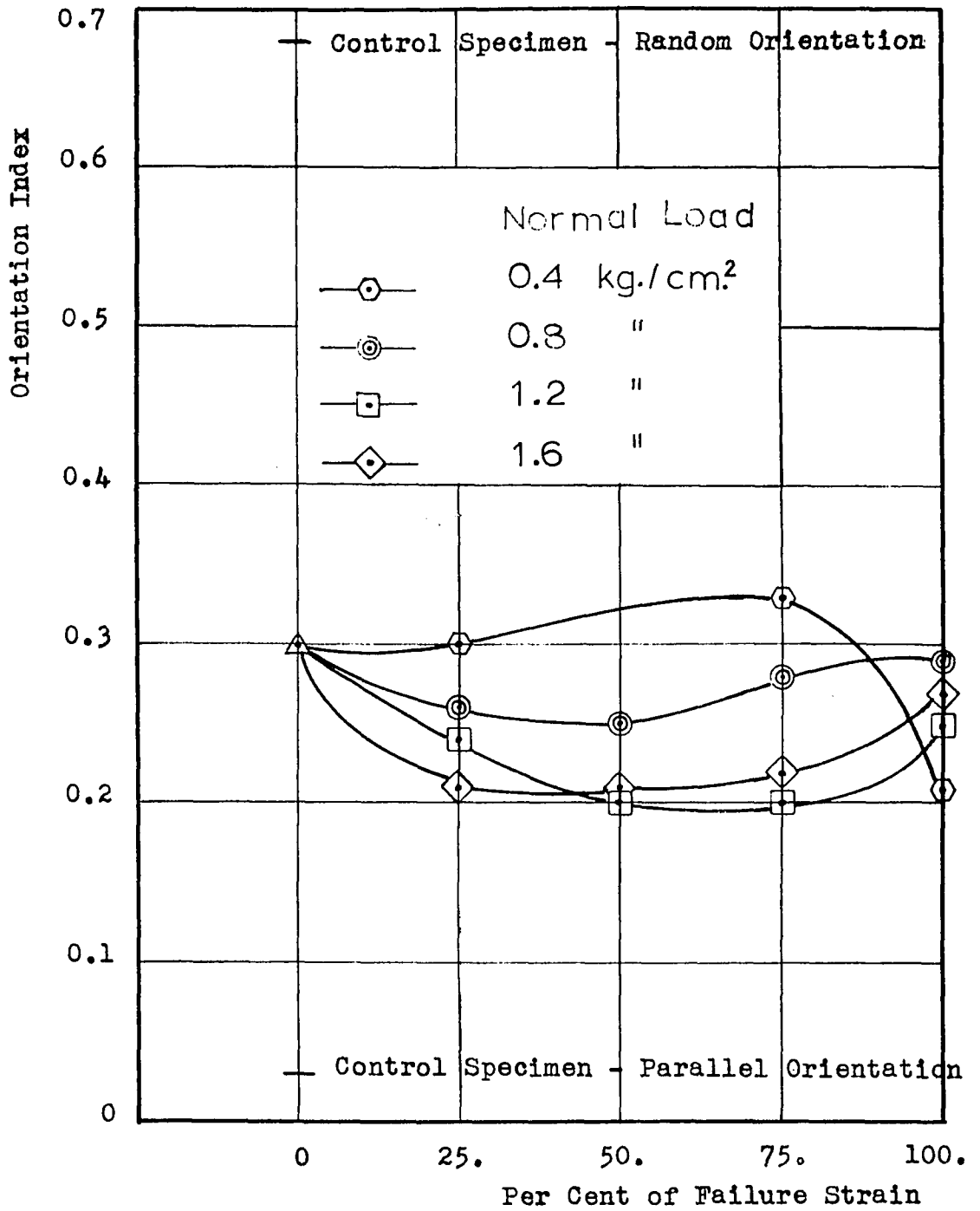


Figure 10

Variation of Orientation Index With Per Cent of Failure Strain - Horizontal Specimens

that the initial fabric of all specimens was of a random orientation. Figures 9 and 10 show that the fabric was random for the specimen used. From Table 2, page 79, it can be noted that this particular specimen had the highest molding moisture content (low of optimum) of all of the specimens used. Therefore, it is safe to assume that because its fabric was randomly-oriented, the fabric of specimens molded at a lower moisture content will also be randomly-oriented.

3) Perhaps the most significant feature of the curves in Figures 9 and 10 is that they do not conform to the generally accepted postulate that shear strains cause a gradual, uni-directional trend toward parallelism of individual clay particles. In general, the curves suggest that initially there is a trend toward parallelism, although the use of only one specimen for the initial condition seriously limits the validity of this observation. The curves do, however, indicate that a fabric change does take place with increasing shear strain. Furthermore, the data suggest that the change is not uni-directional toward a more parallel orientation, but at some point in the shearing process there is a tendency toward randomness. Finally, it is difficult to establish whether or not the variation of orientation index with increasing strain as shown in Figures 9 and 10 is a function of the normal load. The amount of data represented by the curves does not warrant considering the curves as members of the same "family". A possible explanation for

the phenomena shown in Figures 9 and 10 is that the strain distribution within a circular shear specimen, across the specimen normal to the direction of the applied shear load is non-linear (Figure 17, Appendix C, page 83). A non-linear strain distribution of this type, even in an homogeneous material, would produce a complex failure surface. For non-homogeneous specimens such as the kaolinite specimens used in this study the complexity of the three-dimensional failure surface is increased. In addition to the horizontal "dish-type" failure surface expected to result from the non-linear strain distribution in a circular shear specimen, density gradients, formed during the shearing process, add vertical non-linearities to the already complex failure surface (Figure 7(a), page 33). The result of the interaction of these two factors is the development of a highly-complex three-dimensional failure surface. The effect on the fabric of the clay material during shear is not yet fully understood. It is apparent from the above discussion and from the results of the electron microscope study presented later that for circular specimens the failure surface is quite complex and must be properly considered in three dimensions. It is not surprising that the fabric changes accompanying shear strains under these conditions do not conform to those postulated for a simpler two-dimensional model.

Another possible explanation for the shape of the curves in Figures 9 and 10 did not become apparent until after the electron microscope study had been completed. This explanation will be discussed as part of the results of that study.

The Electron Microscope Study

The electron microscope study was performed for the following purposes: to clarify and substantiate the results of the x-ray diffraction data by actual observation of fabric changes resulting from shear strain; to record the observed fabric changes photographically as electron micrographs; to determine quantitatively the size of the shear zone; and to qualitatively describe its internal composition by analysis of the electron micrographs and by direct observation of selected replicas in the electron microscope.

A Presentation of the Electron Micrographs

The electron micrographs shown in Figures 11 through 15, pages 56 through 60, will be used in the discussion of each phase of the electron microscope study. All micrographs have the following features in common:

- 1) The scale shown on each micrograph represents a length of one micron.
- 2) The vertical specimen is always shown above the horizontal specimen.

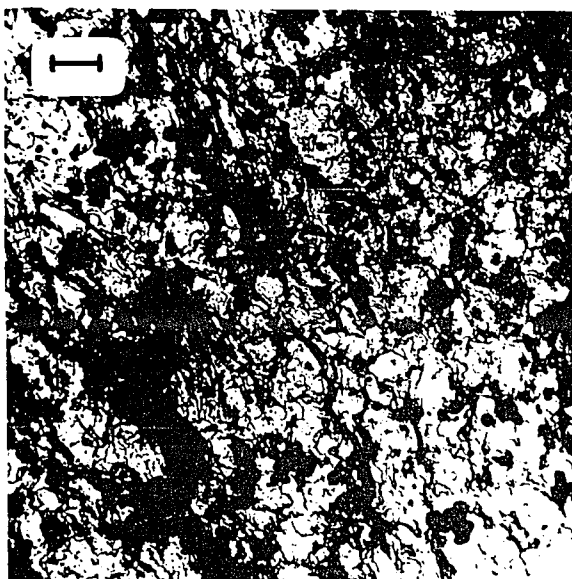
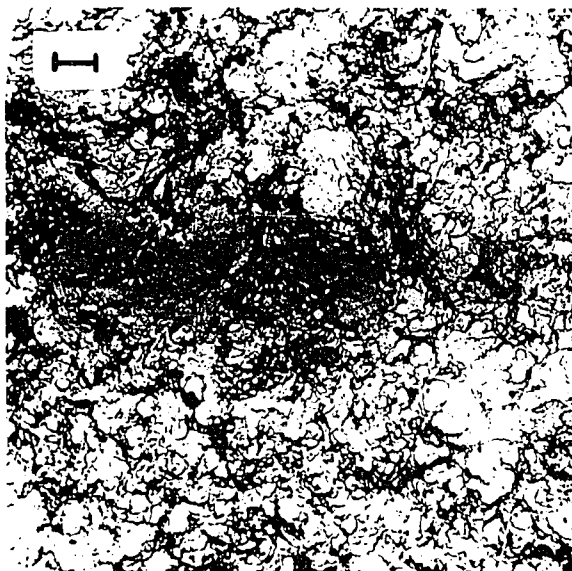


Figure 11

Kaolinite Fabric - Initial Condition
Vertical Specimen (Above)
Horizontal Specimen (Below)

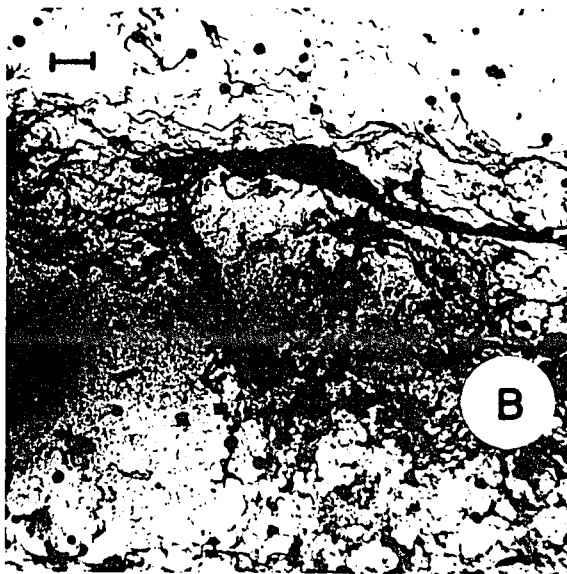
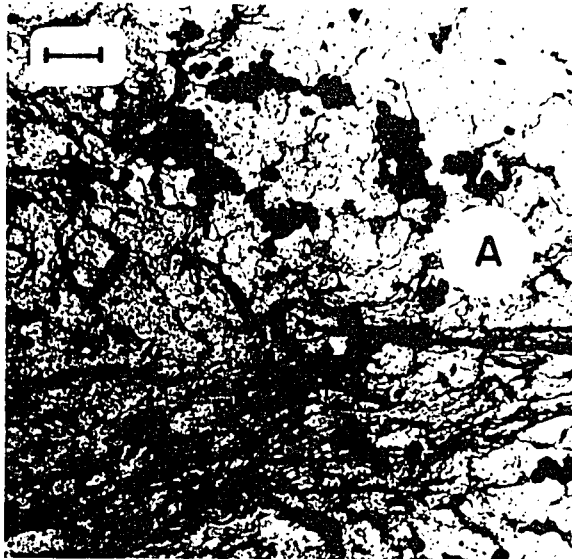


Figure 12

Kaolinite Fabric - 25 Per Cent of Failure Strain
Vertical Specimen (Above)
Horizontal Specimen (Below)

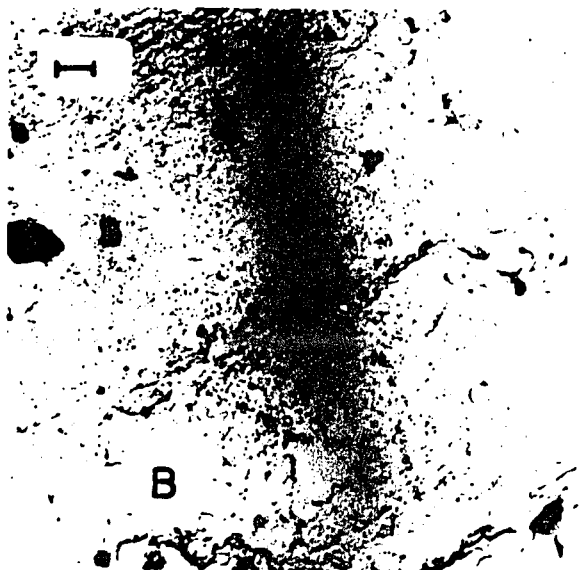
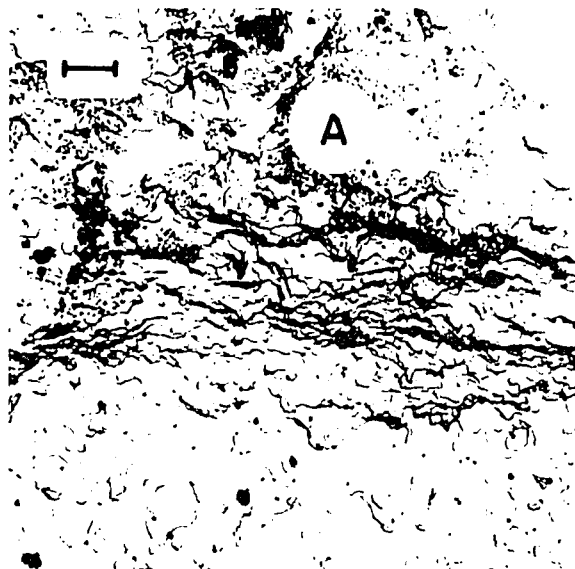


Figure 13

Kaolinite Fabric - 50 Per Cent of Failure Strain
Vertical Specimen (Above)
Horizontal Specimen (Below)

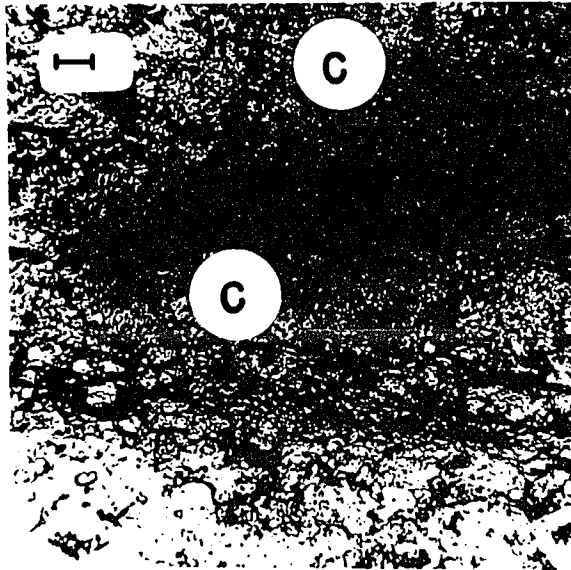
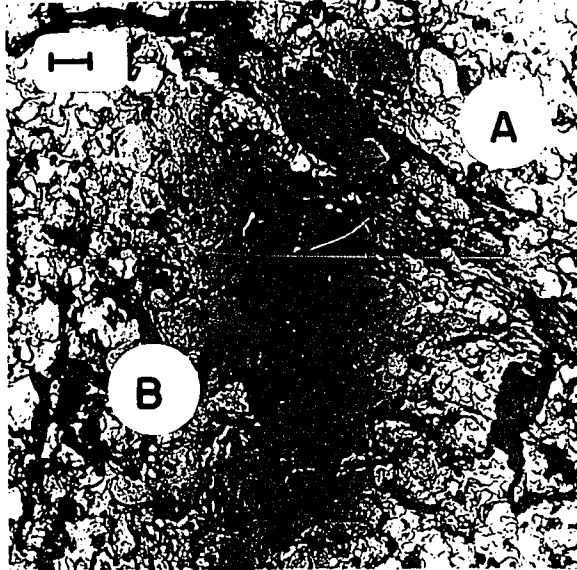


Figure 14
Kaolinite Fabric - 75 Per Cent of Failure Strain
Vertical Specimen (Above)
Horizontal Specimen (Below)

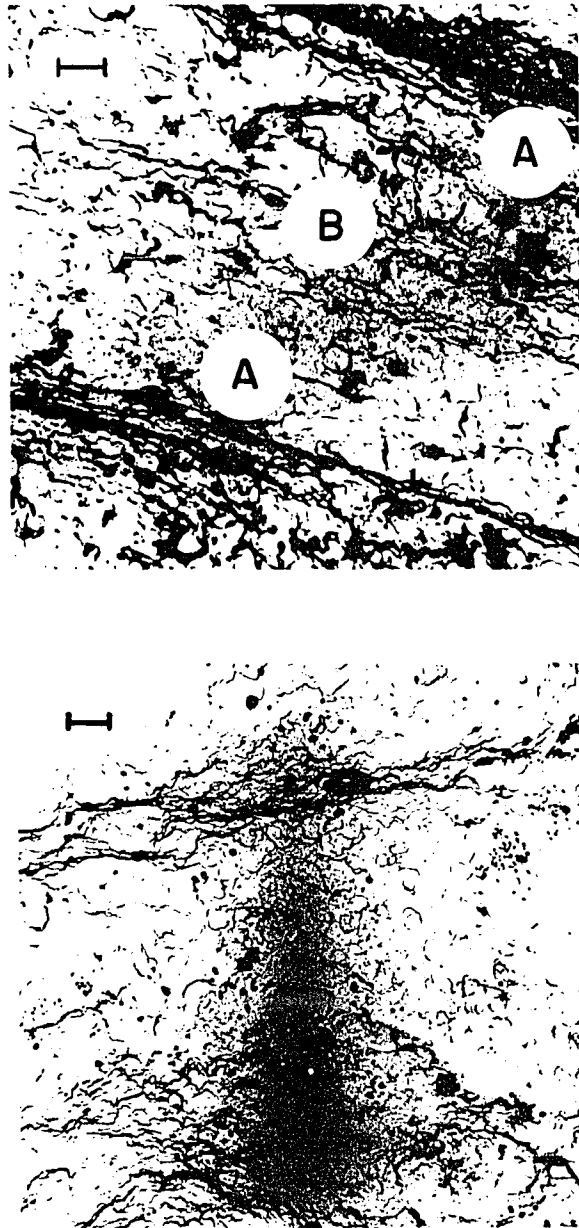


Figure 15

Kaolinite Fabric - Failure Condition
Vertical Specimen (Above)
Horizontal Specimen (Below)

3) Except for the 75 and 100 per cent failure-strain specimens, the orientation of the micrographs with reference to the position of the specimen in the shear box is: (a) for the vertical view, the top of the specimen is toward the top of the page and the front of the specimen away from the binding edge; (b) for the horizontal view, the outside of the specimen is toward the bottom of the page and the front of the specimen away from the binding edge.

For a clearer explanation of the terms "top", "front", and "outside" see Figure 8, page 41. In Figures 14 and 15, pages 59 and 60, for the 75 and 100 per cent failure-strain specimens respectively, the "front" in both the vertical and horizontal views is toward the binding edge; the "top" and "outside" are the same as for the other specimens.

Quantitative and Qualitative Analysis of the Shear Zone

The size of the shear zone was quantitatively determined using the procedure described in Chapter II. The values reported in Table 5, page 62, for each strain condition are an average of values obtained by viewing different areas of the same replica and by viewing other replicas at the same strain condition.

TABLE 5	
Approximate Size Of Shear Zone Along Vertical Diametrical Plane Parallel To Applied Shear Load	
Specimen	Size of Shear Zone In Microns
25V 1.2	790
50V 1.2	1165
75V 1.2	1250
100V 1.2	1324

The shear zone was considered as that zone in which any noticeable degree of reorientation of fabric had occurred. Its extent was often quite difficult to define precisely because of the slight reorientation that was characteristic at the boundaries. Consequently, the values given in Table 5 above, are approximations, and refer only to the vertical extent of the shear zone on the diametrical plane parallel to the applied load.

From the values in Table 5 it is apparent that the vertical extent of the gross shear zone has been almost fully established between 25 and 50 per cent of failure strain. The rate of increase in the vertical extent of the gross shear zone after 50 per cent strain has been reached is almost negligible when compared to the rate of increase up to 50 per cent strain. The significant changes in the shear zone that take place after 50 per cent strain are principally internal changes within the fabric of the gross shear zone rather than external changes in vertical extent.

The electron micrographs in Figure 11, page 56, show that for the zero shear-strain condition the fabric is, in general, random in both the vertical and horizontal views.

Figure 12, page 57, shows that after 25 per cent strain a reorientation is evident in the vertical view and an oriented zone (A) has formed in the direction of the applied shear load. The horizontal view is characterized by the formation of a terrace-like oriented zone (B), also approximately parallel to the applied shear load, with the higher part of the terrace toward the "outside" of the specimen.

The vertical view in Figure 13, page 58, shows that after 50 per cent strain there exists an oriented zone (A)

somewhat larger in size than the similar zone shown in Figure 12, but more inclined to the axis of the applied shear load. The parallel orientation within (A) is also better developed. The horizontal view in Figure 13, page 58, shows that there has been an increase in the number of terrace-like oriented zones but that they still lie approximately parallel to the direction of applied shear and that the highest terrace (B) is still toward the outside of the specimen.

It is not observable in individual electron micrographs, but the characteristic change that has taken place in the process of going from 0 to 50 per cent failure strain is one of increase in the size of the gross shear zone. The areal extent of the gross shear zone which contains individually-oriented zones of the type shown in Figures 12 and 13, pages 57 and 58, has increased. The fabric between these zones and the size of the individually-oriented zones, once formed, has not changed significantly with increase in shear strain up to 50 per cent of failure strain.

Observation of replicas of specimens at strains greater than 50 per cent failure strain and the electron micrographs shown in Figures 14 and 15, pages 59 and 60, indicate that changes of a different nature have taken place. From Table 5, page 62, it can be seen that there is no significant change in the vertical extent of the gross shear

zone after 50 per cent failure strain has been reached. The vertical view in Figure 14, page 59, of the 75 per cent failure-strain specimen shows that massive reorientation has taken place between individually oriented zones so that it is hard to distinguish one zone (A) from another (B). The zones themselves are more inclined to the direction of applied shear load than those shown in any of the previous electron micrographs. The horizontal view of Figure 14, page 59, shows the same massive reorientation taking place between terraces(C).

Finally, in Figure 15, page 60, it can be seen from the vertical view that at 100 per cent failure-strain the number of individually-oriented zones (A) has increased, that the parallel orientation within these zones is very highly developed, and that the fabric between these zones shows definite signs toward parallelism (B). The angular rotation of the zones with respect to the axis of shear loading is greatest. The horizontal view in the same figure shows that the terracing has been so widely extended that a "dish-shaped" failure surface begins to be evident. The higher portion of the dish is toward the "outside" of the specimen.

From Figures 11 through 15 it is apparent that shear strains affect a randomly-oriented clay fabric in the following way:

a) For strains up to approximately 50 per cent of failure, the vertical fabric changes are characterized by the formation and spread of a series of parallel-oriented zones spaced approximately 160 microns apart. The area over which zones of this nature extend increases with increasing strain so that at 50 per cent of failure strain the vertical extent of the shear zone has been almost fully established as approximately 1,300 microns. Also, at 50 per cent of failure strain, the parallelism within the individually-oriented zones has been more fully developed and the vertical extent of the individual zones has increased slightly. In the horizontal direction a similar phenomenon occurs. A series of parallel-oriented terraces form with the higher terraces toward the periphery of the shear specimen. A characteristic feature of the horizontal fabric change is that the terraces have formed throughout the areal extent of the specimen even before 25 per cent of failure strain has been reached. Further straining increases the number of parallel-oriented terraces as well as the degree of orientation within them. At 50 per cent of failure strain the approximate distance between terraces is 5 microns.

b) For strains greater than 50 per cent of failure, the vertical fabric changes are characterized by massive reorientations of previously unaffected areas within the gross shear zone. This orientation results in the formation

of more and more individually-oriented zones. The parallelism within the zones becomes very well-developed. At failure, the distance between these highly parallel-oriented zones is approximately 5 microns, and the fabric between them is no longer randomly oriented. Throughout the shearing process the angular rotation of parallel-oriented zones with respect to the axis of shear load has been increasing, indicative of the effect of density gradients within the shear specimen on the shape of the failure surface. In the horizontal direction the number of terraces has increased to such an extent that it is hard to distinguish between individual terraces. At failure, the shape of the shear zone assumes that of a dish or saucer with the higher portion toward the periphery. Parallelism is also very highly developed.

These concepts of the mechanism governing the development of the shear failure surface seem to contradict those postulated by Yong and Warkentin (1966), however, it would be more appropriate to think of them as a clarification. Instead of the postulation that only one parallel-oriented zone forms and slowly spreads vertically with increase in strain as Yong and Warkentin suggest, the hypothesis advanced above of multiple zone formation within a gross shear zone can be explained more easily from energy considerations. According to Weymouth and Williamson (1953),

"clay particles separated by water films tend to take up positions in a force network such that potential energy is reduced to a minimum. Many particles fail to secure such positions and hence slip is more readily initiated in their vicinity". In an initially randomly-oriented fabric the areas in which particles or groups of particles are in positions of relatively high potential energy are randomly distributed. The force network imposed by the shearing load suggests that the position of maximum potential energy would be a condition of 90°-edge-to-face contact between particles or groups of particles. The shearing force would be normal to the vertical particles. The force network also suggests that the position of minimum potential energy would be complete parallelism between particles or groups of particles in the plane of the shearing load. The above analysis suggests that in the case of a randomly-oriented fabric subjected to pure shear with no normal load the zones of greatest non-parallelism would reorient first, and the reorientation would continue progressively until all zones assumed the same degree of parallelism. Only then would reorientation to parallelism have developed equally throughout the entire sheared mass. The existence of a normal load in the direct shear test and the non-linear nature of the shear strains induced in a circular specimen during the test modify the force network in the following manner:

a) particles or groups of particles closest to the minimum energy position attain that position first. Because both the compressive force and shear force contribute to parallelism, a progressive failure results throughout the gross shear zone in areas where the particle positions are closest to minimum potential-energy states, and

b) in the case of particles or groups of particles in an edge-to-face arrangement, the effect of the compressive force must first be overcome by the shear force before re-orientation to a more parallel position can take place.

The above considerations apply to both the vertical and horizontal zones of shear. The mechanism is further complicated by the non-linearity of the strain distribution in the horizontal plane and by the existence of density gradients in the vertical plane.

A square shear box with teflon coated sides constructed to produce simple shear only (Arthur, James and Roscoe, (1964)) would alleviate the effect of the non-linear strain distribution. A cylindrical, torsion-type shear device (Geuze and Tan, (1953)) might minimize the effect of density gradients. There does not seem to be any single shear device at this time which can surmount both deleterious effects and still yield a potential failure surface that can be located easily.

Correlation of Electron Micrographs With X-ray
Diffraction Data

From the electron microscopy study it can be shown that the random-to-parallel reorientation, which occurs during shear, does not take place in the gradual, progressively-spreading manner formerly thought. That parallel orientation of fabric is effected to a large degree prior to 50 per cent strain is suggested from the results of the x-ray diffraction study shown in Figures 9 and 10, pages 51 and 52. The electron microscope study clearly confirms the x-ray results for both the horizontal and vertical specimens at strains less than 50 per cent of failure strain.

For strains greater than 50 per cent, the x-ray diffraction and electron microscopy evidence seem to contradict one another. For both the horizontal and vertical specimens, the x-ray diffraction results suggest a reorientation of fabric toward randomness while the electron micrographs clearly show the formation of more and more parallel-oriented zones. The apparent contradiction may be resolved by considering the horizontal and vertical specimens separately.

For the horizontal specimens subjected to x-ray diffraction the effect of the vertical density gradient becomes critical at strains greater than 50 per cent of failure. For strains less than 50 per cent of

failure the shape of the shear zone is nearly linear so that the surface of a linear, horizontally-cut section through the zone, when subjected to x-ray diffraction, would be representative of the fabric changes taking place within the zone. By cutting the greater-than-50-per-cent horizontal specimens in the manner shown in Figure 7(b), page 33, a major portion of the surface area subjected to the x-ray beam represents the randomly-oriented zones on both the concave and convex sides of the shear zone. Only a comparatively small area extending radially toward the "outside" of the specimen (refer to Figure 8, page 41,) contains the shear zone. Consequently, after 50 per cent failure strain, the horizontal x-ray diffraction results in Figure 10, page 52, indicate a trend toward randomness. The electron micrographs, on the other hand, clearly show an increase in the number of parallel-oriented terraces and a higher degree of parallelism within the terraces. This apparent contradiction can be explained by closely examining the areas of the horizontal specimens studied in both the x-ray phase and the electron microscopy phase. In the x-ray study the impinging beam covers an area of approximately 2 sq cm, only a small portion of which contains the shear zone. Consequently, the diffracted beam indicates randomness. In the electron microscopy study a replica was made of the central section of the horizontal specimen and was no more than 4 sq mm in size. The

electron micrographs showing parallel-oriented zones indicate that the small portion of the shear zone which appears in the greater-than-50-per-cent horizontal specimens was replicated.

For the vertical specimens subjected to x-ray diffraction the effect of terrace formation and subsequent horizontal "dishing" becomes critical. As shown in Figure 9, page 51, the formation of individually-oriented zones in the vertical direction is suggested by an initial decrease in the orientation index. The subsequent increase in orientation index for most of the specimens may be attributed to the intrusion of parallel-oriented segments of the horizontal shear zone into the vertical plane. The parallel-oriented segments, being part of the "dish-shaped" horizontal surface, appear in the vertical plane at an angle to the axis of the shear load, i.e., the vertical shear zone and the intruded parallel-oriented zones are not mutually parallel. The relative position of these zones changes in a complex manner as strain increases because both the density gradients and the "dishing" effect become more pronounced. The net effect of the intrusion on the x-ray results, however, is that the gross fabric in the vertical sections appears to become more randomly-oriented as strain increases after an initial trend toward parallelism. It is interesting to note that evidence of intrusion can be found in a widening of the (002) peak in the

diffraction trace as the per cent strain increases. Weymouth and Williamson (1953) report the observation by W. Riedel of a similar phenomenon during the direct shear process. Riedel gave the name "slip joints" to the intersection of two individually-oriented zones. It is difficult to say whether or not the "slip joint" can be attributed to the same factors as postulated above because the test conditions in each study were different.

The electron microscopy study supports the hypothesis presented above. From Figures 13 through 15, pages 58 through 60, it is evident that the angular position of the parallel-oriented areas increases with reference to the axis of the applied shear load. When some of the electron micrographs of vertical sections (not shown in Figures 11 through 15) were first viewed, and the top and front of the specimen located on them, it was thought that the replica had been severely rotated during the mounting procedure. The angle between the parallel-oriented zones and the axis of shear was in excess of 45° . It is now apparent that the parallel-oriented zones at such large angles may not have been parallel-oriented zones in the vertical direction affected by density gradients as originally thought, but that they were higher-angle intrusions from the horizontal shearing plane.

CHAPTER IV

CONCLUSIONS AND RECOMMENDATIONS FOR FURTHER STUDY

Conclusions

1) The fabric-reorientation mechanism in a partially-saturated kaolinite clay, subjected to increasing shear strain, is shown diagrammatically in Figure 16. The reorientation takes place through the formation of a series of individually parallel-oriented zones within a gross shear zone. Although Figure 16 shows only the vertical fabric change, the same fabric-reorientation mechanism also operates horizontally. The observed multiple zone formation within a gross shear zone is explained by considering the total strain energy and its effect on the potential energy states of the particle packets constituting the fabric.

2) The vertical extent of the gross shear zone is almost fully established between 25 and 50 per cent of failure strain. At failure, the vertical extent of the gross shear zone measures approximately 1.5 cm at the center of the specimen.

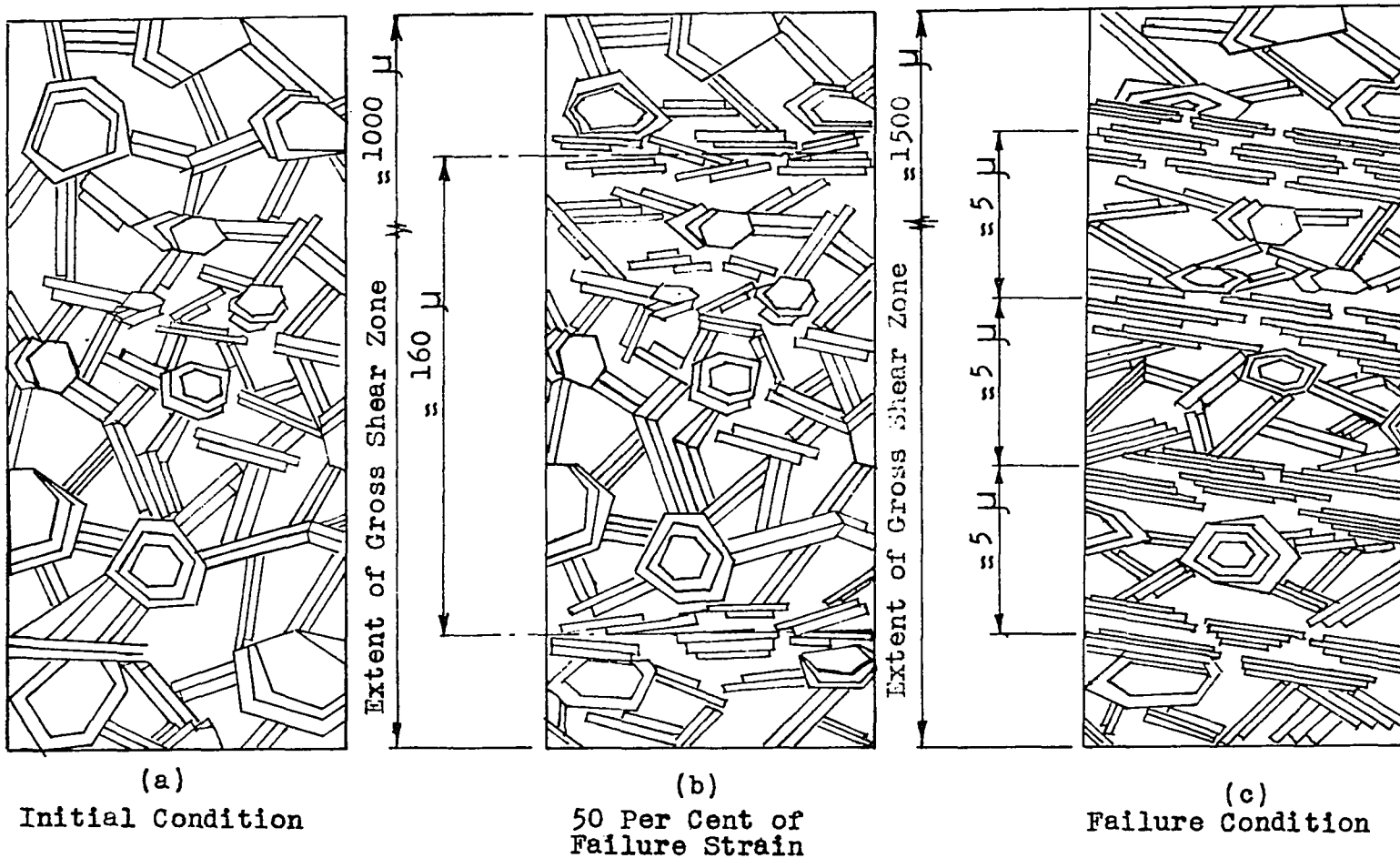


Figure 16

Vertical Fabric Reorientation Due to Increasing Shear Strain

3) The horizontal extent of the gross shear zone is fully established before 25 per cent of failure strain and extends throughout the specimen.

4) The complex three-dimensional failure surface, characteristic in the direct shear of circular specimens, contributes to an interaction of fabric changes in the horizontal and vertical directions.

5) X-ray diffraction and electron microscopy are mutually complimentary methods for the study of the fundamental soil property—fabric.

Recommendations For Further Study

The results of this study offer a basis from which to proceed into a broader investigation of the effects of shear strain on the fabric of cohesive soils. It appears that further research should be directed along the following paths:

1) To investigate the fabric reaction to shear strain of other clays with different physico-chemical properties. A corrolary to this would be to investigate the fabric reaction to shear strain of natural fine-grained soils.

2) To study the effect of shear strain on specimens fully saturated after molding.

3) To investigate the fabric reaction to changes in normal load. It was the original intent of this study to

investigate this area, but time limitations prevented so ambitious an undertaking.

4) To use a plane strain or simple shear device and square specimens to offset three-dimensional influences.

5) To examine the effect of extreme environmental changes on fabric reaction to shear strains for possible application to lunar and planetary soils.

6) To study the effect of shear strain on pore fabric.

X-ray diffraction and electron microscopy seem ideally suited to fabric studies and, therefore, are recommended as the basic research tools for the foregoing suggested future research.

APPENDIX A

TABLES RELATING TO PHYSICAL PROPERTIES OF HYDRITE UF

TABLE 1

Physical Properties of Hydrite UF*

Liquid Limit = 52

Plastic Limit = 34

Plasticity Index = 18

Shrinkage Limit = 37

Specific Gravity of Solids = 2.62

Natural Water Content = 0.44%

Particle Size = -2 microns

p^H = 4.2

* Kaolinite from the Georgia Kaolin Co., Dry Branch, Georgia.

TABLE 2

Molding Moisture Content and Dry Density Values
For Kaolinite Shear Samples

Sample Number*	Molding Moisture Content (%)	Dry Density lbs/cu ft
100	31.5	84.0
75	32.6	86.7
50	31.6	84.2
25	32.4	85.8
0	32.6	86.4

* The sample number indicates the per cent of failure strain to which the sample was eventually subjected.

APPENDIX B

PERTINENT X-RAY DIFFRACTION DATA

TABLE 4

Pertinent Results Computed From Peak Counts For Both
Carbowax-impregnated Test Specimens And Non-impregnated
Control Specimens.

Specimen	Avg.Count (020)*	Std.Dev. (020)	Avg.Count (002)	Std.Dev. (002)
100VO.4	152.	6.202	328.	12.379
75VO.4	145.	4.440	304.	6.558
50VO.4	**			
25VO.4	147.	5.655	372.	12.870
100HO.4	85.	4.024	390.	5.582
75HO.4	136.	4.486	401.	7.893
50HO.4	**			
25HO.4	134.	3.913	438.	7.830
100VO.8	151.	4.895	301.	6.141
75VO.8	148.	4.700	308.	5.892
50VO.8	155.	4.342	341.	6.558
25VO.8	149.	4.233	365.	8.581
100HO.8	98.	3.089	335.	5.428
75HO.8	130.	4.882	460.	11.088
50HO.8	125.	4.822	484.	7.963
25HO.8	124.	5.160	468.	18.575
100V1.2	128.	4.361	339.	18.814
75V1.2	140.	3.941	304.	6.484
50V1.2	164.	4.961	292.	5.799
25V1.2	165.	4.983	326.	5.460
100H1.2	94.	3.557	374.	7.890
75H1.2	111.	6.488	549.	28.679
50H1.2	116.	4.957	561.	21.726
25H1.2	122.	4.557	498.	13.400

* Indices of crystal planes investigated shown in parentheses.

** Data missing due to error in specimen-cutting procedure.

TABLE 4--Continued

Specimen	Avg.Count (020)*	Std.Dev. (020)	Avg.Count (002)	Std.Dev. (002)
100V1.6	145.	4.342	300.	5.261
75V1.6	148.	4.611	304.	6.928
50V1.6	161.	4.969	317.	6.608
25V1.6	157.	5.464	349.	5.667
100H1.6	94.	4.357	344.	5.860
75H1.6	116.	7.012	521.	26.764
50H1.6	115.	3.715	541.	10.206
25H1.6	116.	5.056	548.	15.839
IC-VO.0	160.	5.074	333.	10.954
IC-HO.0	133.	3.955	434.	5.485
Ideal Randomly- Oriented	111.	4.364	162.	5.443
Parallel- Oriented	36.	3.162	1,074.	9.325

* Indices of crystal planes investigated shown in parentheses.

APPENDIX C

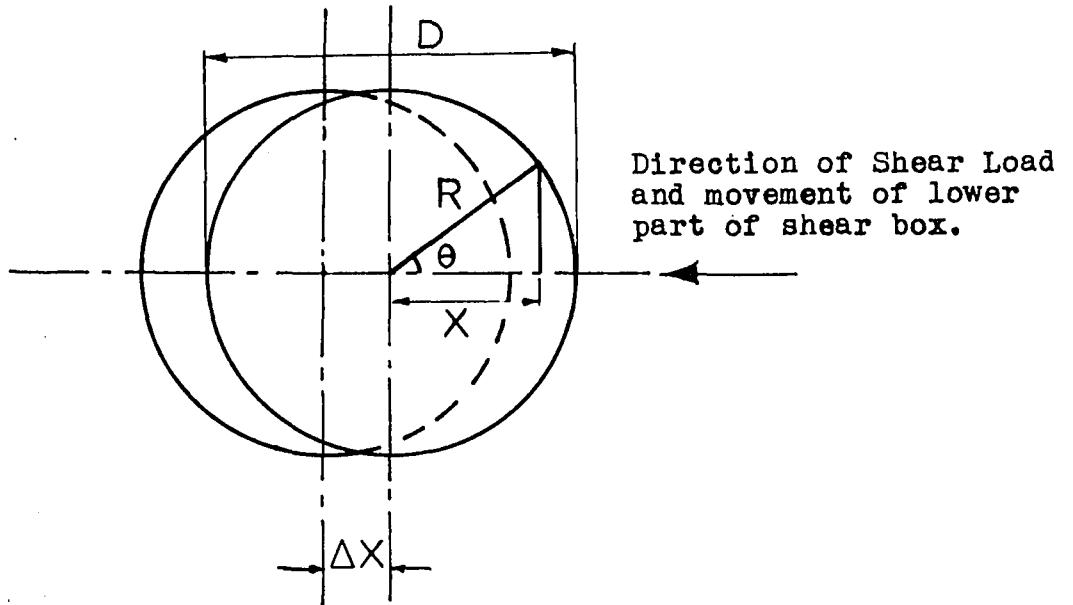
BASIS FOR NON-LINEAR NOMINAL STRAIN
DISTRIBUTION IN A CIRCULAR SHEAR SPECIMEN

BASIS FOR NON-LINEAR NOMINAL STRAIN
DISTRIBUTION IN A CIRCULAR SHEAR SPECIMEN

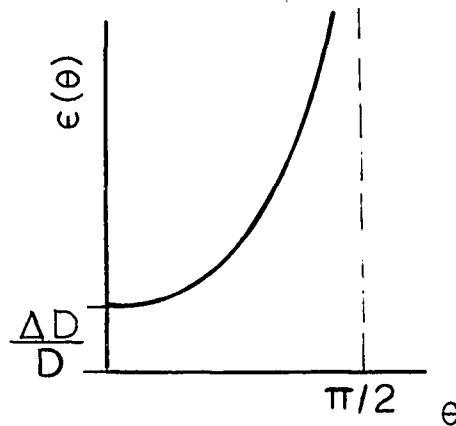
The nominal shear strain shown in Figure 17(a) is defined as

$$\epsilon = \frac{\Delta X}{2 \cdot X} = \frac{\Delta X}{2R \cdot \cos \theta} = \frac{\Delta X}{D} \cdot \sec \theta \quad (8)$$

From Figure 17(b) it is apparent that the shear strain is minimum on the diameter parallel to the axis of the applied shear load and that it is equal to $\Delta D/D$. The shear strain is theoretically infinite at the edge 90° from the axis of the applied shear load. The material at the edge is strained beyond its failure point, therefore, the theory does not apply. The strain distribution is non-linear as shown in Figure 17(b).



(a)



(b)

Figure 17

Non-linear Nominal Strain Distribution
in a Circular Specimen

LIST OF REFERENCES

- Arthur, J.R., R.G. James and K.H. Roscoe (1964), The determination of stress fields during plane strain of a sand mass, Geotechnique, Vol. 14, No. 4, pp. 283-308.
- Bishop, A.W. (1960a), The principles of effective stress, Publication 32, Norwegian Geotechnical Institute, Oslo: pp. 1-5.
- Bishop, A.W., et al (1960b), Factors controlling the strength of partially saturated cohesive soils, Proceedings, ASCE Research Conference on the Shear Strength of Cohesive Soils, Boulder, Colorado: pp. 503-532.
- Bolt, G.H. (1955), Analysis of the validity of the Gouy-Chapman theory of the electric double layer, Journal of Colloid Sciences, Vol. 10, No. 2, pp. 206-218.
- Bolt, G.H. (1956), Physico-chemical analysis of the compressibility of pure clays, Geotechnique, Vol. 6, pp. 86-93.
- Bradley, D.E. (1954), Evaporated carbon films for use in electron microscopy, British Journal of Applied Physics, Vol. 5, No. 2, pp. 65-66.
- Casagrande, A. (1932), The structure of clay and its importance in foundation engineering, Journal, Boston Society of Civil Engineers, Vol. 19, pp. 168-209.
- Casagrande, A. (1960), Structure and volume of voids of soils, From Theory to Practice in Soil Mechanics, John Wiley & Sons, New York: pp. 146-148.
- Geuze, E.C. and T.K. Tan (1953), The mechanical behavior of clays, Proceedings, 2nd International Congress on Rheology, Oxford: pp. 247-259.
- Grim, R.W. (1942), Modern concepts of clay minerals, Journal of Geology, Vol. 50, No. 3, pp. 225-275.
- Henkel, D.J. (1959), The relationships between the strength, pore-water pressure, and volume-change characteristics of saturated clays, Geotechnique, Vol. 9, pp. 119-135.

LIST OF REFERENCES Continued

- Henkel, D.J. (1960), The relationships between the effective stresses and water content in saturated clays, Geotechnique, Vol. 10, pp. 41-54.
- Hvorslev, M.J. (1938), The shearing resistance of remolded cohesive soils, Proceedings of the Soils and Foundation Conference, U.S. Engr. Dept., Boston: Section E, 30 pp.
- Hvorslev, M.J. (1960), Physical components of the shear strength of saturated clays, Proceedings, ASCE Research Conference on the Shear Strength of Cohesive Soils, Boulder, Colorado: pp. 169-274.
- Kell, T.R. (1964), The influence of compaction method on the fabric of compacted clay, M.S. Thesis, The University of Arizona.
- Lambe, T. W. (1953), The structure of inorganic soil, Proceedings Separate 315, ASCE, Vol. 79.
- Lambe, T.W. (1958a), The structure of compacted clay, Journal, Soil Mechanics and Foundations Division, ASCE, Vol. 84, No. SM 2.
- Lambe, T.W. (1958b), The engineering behavior of compacted clay, Journal, Soil Mechanics and Foundations Division, ASCE, Vol. 84, No. SM 2.
- Martin, G.L. (1965), The consolidation process in a partially saturated clay, PhD. Dissertation, The University of Arizona.
- Martin, R.T. (1965), Quantitative fabric of consolidated kaolinite, Phase Report No. 4, Department of Civil Engineering Publication R65-47, MIT.
- Michaels, A.S. and C.S. Lin (1955), Effects of counter-electro-osmosis and sodium ion exchange on the permeability of kaolinite, Industrial and Engineering Chemistry, Vol. 47, Pt. 1, No. 6, pp. 1249-1253.
- Mitchell, J.K. (1956), The fabric of natural clays and its relation to engineering properties, Proceedings, Highway Research Board, Nat'l. Acad. Sci.-Nat'l. Res. Council, Washington, D.C., Vol. 35, pp. 693-713.

LIST OF REFERENCES Continued

- Mitchell, J.K. (1960), Components of pore water pressure and their engineering significance, Proceedings, 9th National Conference on Clays & Clay Minerals, Pergamon Press, Oxford: pp. 162-184.
- Olsen, R.E. (1963), Shear strength properties of sodium illite, Journal, Soil Mechanics and Foundations Division ASCE, Vol. 89, SM 1, pp. 183-208.
- Parry, R.H.G. (1959), Latent interparticle forces in clays, Nature, Vol. 183, No. 4660, pp. 538-539.
- Rendulic, L. (1937), Ein grundgesetz der tonmechanik und sein experimenteller beweis, Bauingenieur, Berlin: Vol. 18, pp. 459-467.
- Roscoe, K.H., A.N. Schofield and C.P. Wroth (1958), On the yielding of soils, Geotechnique, Vol. 8, pp. 22-53.
- Rosenqvist, I. Th. (1955), Investigations in the clay-electrolyte-water system, Publication No. 9, Norwegian Geotechnical Institute, Oslo.
- Rosenqvist, I.Th. (1957), Soil properties and their measurement, Proceedings, 4th International Conference on Soil Mechanics and Foundation Engineering, London: Vol. II, pp. 427-432.
- Russell, E.W. (1934), The interaction of clay with water and organic liquids as measured by specific volume changes and its relation to the phenomena of crumb formation in soils, Philosophical Transactions, Royal Society of London, Vol. 233, pp. 361-389.
- Scott, R.F. (1963), Principles of Soil Mechanics, Addison-Wesley Publishing Co., Reading, Pa.: pp. 336-395.
- Seed, H.B. and C.K. Chan (1959a), Structure and strength characteristics of compacted clays, Journal, Soil Mechanics and Foundations Division, ASCE, Vol. 85, SM 5, pp. 87-128.
- Seed, H.B. and C.K. Chan (1959b), Undrained strength of compacted clays after soaking, Journal, Soil Mechanics and Foundations Division, ASCE, Vol. 85, SM 6, pp. 31-47.

LIST OF REFERENCES Continued

- Tan, T.K. (1957), Discussion on structure and rheological properties of soils, Proceedings, 4th International Conference on Soil Mechanics and Foundation Engineering, London: Vol. 3, pp. 278-279.
- Ter-Stepanian, G. (1936), On the influence of scale-like shape of clay particles on the process of shear in soils, Proceedings, 1st International Conference on Soil Mechanics and Foundation Engineering, Harvard University, Vol. 2, pp. 112-116.
- Terzaghi, K. (1925), Erdbaumechanik auf Bodenphysikalische Grundlage, Deuticke, Leipzig, 399 pp.
- Warshaw, C.M. and R.Roy (1961), Classification and a scheme for the identification of layer silicates, Bulletin, Geological Society of America, Vol. 72, pp. 1455-1492.
- Weymouth, and W.O. Williamson (1953), The effect of extrusion and some other processes on the micro-structure of clay, American Journal of Science, Vol. 251, pp. 89-108.
- Winterkorn, H.F. and G.P. Tschebotarioff (1947), Sensitivity of clay to remolding and its possible causes, Proceedings, Highway Research Board, Nat'l. Acad. Sci.-Nat'l. Res. Council, Washington, D.C., Vol. 27, pp. 435-442.
- Yong, R.N. and B.P. Warkentin (1966), Introduction to Soil Behavior, The Macmillan Company, New York: pp. 314-320.